GABA B receptor cell-surface export is controlled by an endoplasmic reticulum gatekeeper

Stéphane Doly, Hamasseh Shirvani, Gabriel Gäta, Frank J Meye, Michel-Boris Emerit, Hervé Enslen, Lamia Achour, Liliana Pardo-Lopez, Seung-Kwon Yang, Vincent Armand, et al.

$GABA_B$ receptor cell surface export is controlled by an endoplasmic reticulum gatekeeper

Stéphane Doly[1,2,3]*, Hamasseh Shirvani[1,2,3]*, Gabriel Gäta[1,2,3,4], Frank J. Meye[5], Michel-Boris Emerit[3,6], Hervé Enslen[1,2,3], Lamia Achour[1,2,3], Liliana Pardo-Lopez[1,2,3,§], Seung-Kwon Yang[3,6], Vincent Armand[3,6], Robert Gardette[3,6], Bruno Giros[7,8], Martin Gassmann[9], Bernhard Bettler[9], Manuel Mameli[5], Michèle Darmon[3,6], Stefano Marullo[1,2,3].

1: INSERM, U1016, Institut Cochin, Paris, France

2: CNRS, UMR8104, Paris, France

3: Université Paris Descartes, Sorbonne Paris Cité, France

4 : Université Paris Diderot, Sorbonne Paris Cité, France

5. Institut du Fer a Moulin, INSERM UMR-S 839, Université Pierre et Marie Curie, Paris France.

6 : INSERM U894, Centre de Psychiatrie et Neurosciences, Paris, France

7: INSERM U952, CNRS UMR 7224, Université Pierre et Marie Curie, Physiopathologie des Maladies du Système nerveux Central, Paris, France

8. Douglas Hospital Research Center, Department of Psychiatry, McGill University, Montreal, QC, Canada

9. Department of Biomedicine, University of Basel, Basel, Switzerland

*Equally contributed

§ Present address: Instituto de Biotecnología, Universidad Nacional Autónoma de México, Cuernavaca, Morelos México.

Corresponding author: Stefano Marullo, Institut Cochin, Paris, France

stefano.marullo@inserm.fr

Tel (33) 1 40 51 65 52; Fax (33) 1 40 51 65 91

Summary

Endoplasmic reticulum (ER) release and cell surface export of many G protein-coupled receptors (GPCRs), are tightly regulated. For $GABA_B$ receptors of GABA, the major mammalian inhibitory neurotransmitter, the ligand-binding GB1 subunit is maintained in the ER by unknown mechanisms in the absence of hetero-dimerization with the GB2 subunit. We report that GB1 retention is regulated by a specific gatekeeper, PRAF2. This ER resident transmembrane protein binds to GB1, preventing its progression in the biosynthetic pathway. GB1 release occurs upon competitive displacement from PRAF2 by GB2. PRAF2 concentration, relative to that of GB1 and GB2, tightly controls cell surface receptor density and controls $GABA_B$ function in neurons. Experimental perturbation of PRAF2 levels *in vivo* caused marked hyperactivity disorders in mice. These data reveal an unanticipated major impact of specific ER gate-keepers on GPCR function and identify PRAF2 as a new molecular target with therapeutic potential for psychiatric and neurological diseases involving $GABA_B$ function.

Introduction

Cellular responses to hormones and neurotransmitters depend on the cell surface density of cognate receptors. Surface receptor number can vary considerably during adaptive responses to specific physiological constraints and in pathological conditions, both because of altered endocytosis [1] and changes in trafficking of receptors to the plasma membrane [2]. These processes have been intensively investigated for heptahelical receptors (also known as G protein-coupled receptors or GPCRs), which represent the largest family of plasma membrane receptors. For several GPCRs, the largest proportion of receptor molecules is not at the plasma membrane of native cells, but instead within internal stores [3-7]. Receptors can be mobilized from these stores upon external stimuli [4, 8, 9] targeting key components of the secretory pathway [10], or after binding to endogenous ligands, which exert a chaperoning effect [11]. The cell surface delivery of these GPCRs is facilitated by a complex network of interactions with specific cellular chaperones or escort proteins [5-7, 12-15], which allow the egress of receptors from the endoplasmic reticulum (ER) or release from the Golgi apparatus. Despite the identification of sequence motifs on cargo receptors, which control capture or release from intracellular stores, the molecular mechanisms of receptor retention are poorly understood. COP1 coatomer-dependent retrieval from the cis-Golgi to the ER was proposed in some cases [16, 17], whereas retention via specific interaction with a ER resident gate-keeper was only reported during early development for Frizzled, a GPCR involved in the Wnt signaling pathway [18].

Gamma-aminobutyric acid (GABA) is the principal inhibitory neurotransmitter in the vertebrate central nervous system. Its metabotropic $GABA_B$ receptor is a prototypical paradigm of an intracellularly-retained GPCR with regulated cell-surface

export [19]. Functional $GABA_B$ receptors are hetero-dimers constituted of two receptor protomers, referred to as GB1 and GB2 [20-22]. Two GB1 isoforms (GB1a and GB1b), produced as a consequence of a differential promoter usage in the *GB1* gene [23], differ in their ectodomains by a pair of sushi repeats, which localize $GABA_B$ receptors to distinct synaptic sites, are. Although containing the GABA binding site in the extracellular domain [20], GB1 isoforms fail to reach the cell surface when expressed in heterologous systems or overexpressed in neurons [24]. Indeed, GB1 contains an arginine-based signal in its carboxy-terminal tail, which causes its retention in the ER [25, 26], and a di-leucine motif, which controls GB1 interaction with a guanine-nucleotide exchange factor and its exit from the trans-Golgi network [27]. GB2, on the other hand, does not bind to any known $GABA_B$ ligand [28] but is responsible for G-protein coupling [29, 30]. GB2 does not contain any retention signal and can reach the cell surface in the absence of GB1, as a functionally inactive homo-dimer [31]. It has been proposed that the shielding of the GB1 retention signal via a coiled-coil interaction with the carboxy-terminal of GB2 allows the hetero-dimer to reach the cell surface [25], but the mechanistic aspects underlying GB1 retention have remained elusive. Although several proteins have been reported to interact with the coiled-coil domain of GB1 and to somehow regulate $GABA_B$, none of them plays a direct role in GB1 retention in the ER: 14-3-3ζ disrupts GB1-GB2 heterodimers at the cell surface [32]; upregulation of the transcription factor CHOP in response to ER stress interferes with GB1-GB2 heterodimerization [33]; the ARF1, 3,6 guanine-nucleotide exchange factor msec-7 controls $GABA_B$ exit from the Golgi apparatus [27]; the scaffolding protein GISP enhances $GABA_B$ receptor function by slowing receptor desensitization [34].

Here we identified PRAF2, a 178 amino acid ER-resident protein [35] comprising 4 transmembrane domains with cytosolic amino- and carboxy-termini, as an essential

gatekeeper regulating GB1 release from the ER. PRAF2 is a member of the prenylated rab acceptor family, which includes the two structurally related proteins PRAF1 and PRAF3 [36]. Golgi-resident PRAF1, was proposed to activate the dissociation of prenylated Rab proteins from the GDP dissociation inhibitor GDI, thus facilitating the association of prenylated Rabs with target Golgi membranes [37]. PRAF3, the mammalian analogue of the yeast protein Yip6b, was reported to delay ER exit of the Na^+-dependent glutamate transporter Excitatory Amino-Acid Carrier 1 (EAAC1) [38, 39]. PRAF2 identified in a yeast two-hybrid screen as an interacting partner of the chemokine receptor CCR5 [40], was found enriched in human brain [41] and overexpressed in multiple cancers [36, 42]. However, no specific biological function has so far been attributed to PRAF2.

Our data demonstrate that PRAF2 interaction with GB1 controls $GABA_B$ function at the cell surface of neurons and *in vivo*.

Materials and Methods

Extensive description of materials and methods can be found in Supplementary Material.

Results

PRAF2 interacts with GB1 in the ER of transfected fibroblasts and primary neurons

In the search for a potential gatekeeper retaining GB1 in the ER until it associates with GB2, we investigated whether the ER-resident PRAFs, PRAF2 and PRAF3 might be interacting partners of GB1. Co-immunoprecipitation experiments were conducted in HEK-293 cells expressing tagged proteins. GB1-GFP (the GB1b isoform were used in transfected fibroblasts throughout this study) was found to co-immunoprecipitate (co-IP) with V5-PRAF2, whereas almost no co-IP was observed with V5-PRAF3 (Figure 1a). V5-PRAF2 interacted with GB1 but not GB2 (Supplementary Figure S1a). Based on these observations, subsequent studies focused on PRAF2. To confirm that the interaction between the receptor and PRAF2 occurs in the ER, the glycosylation profile of GB1 that co-immunoprecipitated with PRAF2 was examined (Supplementary Figure S1b). N-glycans added in the ER are sensitive to both Endo H and PNGAse F, whereas subsequent glycosylation in the Golgi is resistant to Endo H and sensitive to PNGAse F [43]. Following co-IP with PRAF2, GB1 was deglycosylated by both enzymes in the presence or absence of co-expressed GB2. In the presence of GB2 most GB1 underwent N-glycosylation in the Golgi, protecting the receptor against Endo H action in the cell lysate (Supplementary Figure S1b, upper panel). These data therefore demonstrate that the GB1, which co-IP with PRAF2 is from the ER and not from post ER compartments.

In agreement with previous studies [36], PRAF2 was found to be present in many cell lines and abundant in the brain (Figure 1b). Likely due to its highly hydrophobic domains, endogenous PRAF2 may form oligomers, which are visible after electrophoretic separation at low stringency [40]. Accordingly, we detected variable combinations of monomeric (≈20kDa) dimeric (≈40kDa) and high molecular weight forms, in rat and mouse tissue or cell extracts and in human cell extracts. In all cases, immunostained material did correspond to PRAF2, as confirmed by the loss of signal following RNA interference (Supplementary Figure S2a).

Endogenous GB1a/GB1b (Figure 1b) and PRAF2 from adult rat brain extracts co-immunoprecipitated (Figure 1c), indicating that both receptor isoforms can be found in a molecular complex with PRAF2. The subcellular distribution of these proteins was studied in embryonic (E17) rat hippocampal neurons grown in culture. Confocal immunofluorescence analysis on permeabilized cells showed marked cytoplasmic co-localization of endogenous GB1 and PRAF2 (80.2±5.6%, Figure 1d). PRAF2 staining was particularly abundant in the cell body, but also present in neurites. GB1 staining (Supplementary Figure S3a for GB1 antibody specificity) overlapped with both ER (KDEL receptor) and Golgi (GM130) markers, whereas PRAF2 was mainly colocalized with the ER marker (76.7±6.7%, Figure 1d), consistent with previous studies [42].

PRAF2 controls GB1 export and regulates $GABA_B$ function at the cell surface of neurons

Based on the experiments above, GB1 and PRAF2 likely interact in the ER, where GB1 is retained in the absence of hetero-dimerization with GB2. To investigate whether PRAF2 could control the exit of GB1 from the ER, hippocampal neurons

were transfected with siRNAs to down-modulate PRAF2 expression. One week after transfection with specific siRNAs, neurons expressed 10-30% residual PRAF2 (Figure 2a and Supplementary Figure S2a). To measure the amount of surface binding sites, binding studies on intact cells were conducted on the same samples using [^{3}H]-CGP54626, a hydrophilic membrane impermeable $GABA_B$ antagonist, which specifically binds to the GB1 isoform and not to GB2 [28] (see also Supplementary Figure S3c). An up to three-fold increase of surface GB1 was measured in cells with decreased PRAF2 expression compared to controls (Figure 2a), consistent with the hypothesis that PRAF2 may function as a GB1 gatekeeper in the ER. In line with this, expression of exogenous PRAF2 in hippocampal neurons following infection with adenoviruses carrying a PRAF2 construct (AAV-PRAF2+GFP) was associated with a 60% decrease of surface GB1 binding sites (Figure 2b). In contrast, and in agreement with their lack of interaction in co-IP experiments, exogenous PRAF2 did not modify the amount of cell surface GB2 in AAV-PRAF2+GFP-infected cells (Supplementary Figure S1c and Supplementary Figure S3b for GB2 antibody specificity).

We next examined whether the additional surface GB1 detected upon PRAF2 inhibition was associated with GB2 within a $GABA_B$ hetero-dimer or released alone. Since $GABA_B$ coupling to G proteins exclusively depends on the GB2 subunit, agonist-promoted functional outputs depend on the formation of $GABA_B$ hetero-dimers [44]. Patch-clamp experiments were therefore conducted to measure the inhibitory effect of the $GABA_B$ agonist baclofen on the spontaneous electric activity of hippocampal neurons in culture (Figure 2c-f, Supplementary Figure S2 and Table S1). The basal spontaneous electrical activity was comparable in untreated neurons, neurons treated with the various siRNAs or infected with AAV-PRAF2+GFP (Figure

2c). Baclofen caused a dose-dependent inhibition of the spontaneous electrical activity of neurons (Figure 2e), the effect being reversed by pre-incubation with the $GABA_B$ antagonist CGP54626 (Figure 2d). Both PRAF2-specific siRNAs led to a leftward shift of the inhibition curve compared to untreated cells or cells receiving scrambled siRNA (Figure 2e), indicating that the inhibition of the spontaneous activity in PRAF2-depleted neurons was much more efficient at lower concentrations of baclofen, as a consequence of an increased number of surface $GABA_B$ hetero-dimers. Conversely, virus-induced overexpression of PRAF2 impaired the effect of baclofen, indicating a decreased number of surface $GABA_B$ hetero-dimers (Figure 2f). Thus, the PRAF2-dependent regulation of GB1 cell surface delivery controls the density of functional $GABA_B$ hetero-dimers, directly impacting on the inhibitory threshold of GABA signaling.

Competition between GB2 and PRAF2 determines the release of GB1 from the ER

The molecular mechanism of GB1 regulation by PRAF2 was investigated in a reconstituted cell model. The cell surface export of GB1 was measured by FACS analysis in transfected HEK-293 cells (see Supplementary Experimental Procedures). In the absence of co-expressed GB2, minor or no amounts of exogenous GB1 are detectable at the surface of transfected cells, depending on the cell type and on the experimental method [25, 26]. Accordingly, in the absence of GB2, extracellular GB1 only represented 5 to 10% of the maximal signal measured upon GB1 and GB2 co-expression in transfected HEK-293 cells (Figure 3a). By increasing the amounts of exogenous PRAF2 in cells expressing constant amounts of GB1 and GB2, a progressive decrease of surface GB1 was observed (Figure 3a). These data suggest that the actual amount of GB1 reaching the cell surface is controlled by GB2

and PRAF2, these proteins exerting opposite effects on forward trafficking. In contrast, PRAF2 was unable to modulate the cell surface targeting of endogenous GB2 in neurons (Supplementary Figure S1c) or exogenous GB2 expressed alone in HEK-293 cells (Supplementary Figure S1d), consistent with the observation that GB2 does not interact with PRAF2 (Supplementary Figure S1a).

Immunofluorescence experiments were then conducted to examine how the subcellular distribution of GB1 is modulated in HEK-293 cells by the co-expression of GB2 and PRAF2 (Supplementary Figure S5). When expressed alone, GB1-GFP was largely intracellular, co-localizing with the ER marker BIP (92.9±1.3%, panels a,f). In the presence of co-expressed GB2-HA, a substantial proportion of GB1-GFP was translocated to the plasma membrane area where it co-localized with GB2-HA (95.4±0.9%, panels b,c,g); if PRAF2-V5 was overexpressed together with GB2-HA, GB1-GFP mostly recovered its original intracellular distribution (80.8±2.6% colocalization with BIP, panels d,h) and appeared less localized with GB2-HA (53.4±3.2%, panel e). Most co-localized PRAF2-V5/GB1-GFP signal also co-localized with the anti-BIP signal (98.1±0.5%, panel d).

These data indicate that the relative stoichiometry of GB1, GB2 and PRAF2 determines the actual amount of surface $GABA_B$ heterodimer, GB2 and PRAF2 competing for GB1 association. The capacity of GB2 to displace the GB1-PRAF2 interaction was assessed by co-IP experiments in the presence of increasing concentrations of GB2: for a constant concentration of PRAF2, increasing GB2 expression progressively reduced the amount of GB1 recovered in complex with PRAF2 (Figure 3b). Bioluminescence Resonance Energy Transfer (BRET) experiments, permit monitoring of the proximity of protein partners in intact cells [45, 46]. PRAF 2 cDNA was fused with the coding region of Renilla luciferase (Rluc), the

BRET donor, and the GB1 coding region was fused upstream to that of the yellow variant (YFP) of the green fluorescent protein (GFP), the BRET acceptor. Saturation BRET experiments [46] were then conducted by transfecting constant amounts of donor plasmid and increasing amounts of acceptor plasmid. Hyperbolic curves indicative of specific GB1-PRAF2 proximity (Figure 3c) were obtained in the absence or presence of increasing amounts of HA-tagged GB2. However, $BRET_{50}$ values, which reflect the propensity of the investigated proteins to be in close proximity, were increased in the presence of HA-GB2, consistent with a model of competitive inhibition of GB1-PRAF2 interaction by GB2. Accordingly, the capacity of GB2 to displace the GB1-PRAF2 interaction was correlated with increased expression of GB1 at the cell surface (Figure 3d).

The RSR motif present in the C-terminus of GB1 participates in its ER retention [25], as shown by the enhanced cell surface expression of the GB1-ASA mutant (alanine substitution of the arginine residues of the RSR motif) even in the absence of GB2 [25-27]. We hypothesized that this RSR motif could participate in the interaction of GB1 with PRAF2. The amount of GB1-ASA co-immunoprecipitated with PRAF2 was decreased compared to wt GB1 (Figure 3e), confirming the above hypothesis, but also indicating that the interface between these proteins may involve other motifs. A di-leucine motif upstream of the RXR motif also participates in the control of cell surface export of GB1, the GB1-AA-ASA mutant (alanine substitution of both RXR and di-leucine motifs), being better exported to the cell surface than wt GB1 or the single GB1-ASA mutant in the absence of GB2 [25]. We compared the interaction of GB1, GB1-ASA GB1-AA and GB1-AA-ASA with PRAF2 in co-IP experiments (Figure 3e) and found that the di-leucine motif participates in the association with PRAF2. The substitution of both LL and RXR motifs abolished the

interaction of GB1 and PRAF2. It was proposed that the LL motif might participate in the interaction of GB1 with a guanine-nucleotide exchange factor in the trans-Golgi network [27]. Our data indicate that the di-leucine motif may also contribute to GB1 retention in the ER.

Increased expression of PRAF2 in ventral tegmental neurons in mice causes major hyperactivity

We next investigated whether perturbing the stoichiometry of GB1, GB2 and PRAF2 might affect $GABA_B$-dependent regulations *in vivo.* $GABA_B$ receptor function was studied in the ventral tegmental area (VTA), a brain area containing $GAGA_B$-expressing neurons [47, 48]. Activation of the dopaminergic circuits from the VTA to the nucleus accumbens produces hyperlocomotor activity [49] and $GABA_B$-mediated activation of slow inhibitory currents plays an important role in the control of dopaminergic neuron excitability in the VTA [48, 50]. Somatodendritic $GABA_B$ receptors inhibit dopamine release by causing K^+-dependent hyperpolarization, which decreases burst firing-activity of dopaminergic neurons [48, 51], whereas presynaptic $GABA_B$ receptors curtail dopamine release by inhibiting Ca^{2+} influx [52]. We predicted that the loss of surface $GABA_B$ receptors in VTA dopaminergic neurons resulting from a local rise in PRAF2 expression and GB1 retention, would contribute to increased dopamine release and subsequent enhanced locomotor activity. Bilateral stereotaxic injection of the bicistronic adenoviral PRAF2 and GFP delivery system (AAV-PRAF2+GFP) into the VTA led to a dramatic dose-dependent increase in basal locomotor activity, compared to animals receiving a virus that only expressed GFP (AAV-GFP) (Figure 4a). Mouse brains were examined to verify the distribution of adenovirus-encoded exogenous PRAF2 and GFP. GFP expression was mostly

restricted to the VTA and occurred in both tyrosine-hydroxylase-positive (dopaminergic) and negative neurons (Supplementary Figure S6a). Habituation to the novel environment had no effect in AAV-PRAF2+GFP-injected mice, whereas AAV-GFP-injected animals showed a progressive reduction in locomotor activity during the session (over the 60min period) and compared to the first day (Figure 4a,b).

To establish the amount of exogenous PRAF2 responsible for these motor phenotypes, PRAF2 was quantified in the VTA by immunoblot experiments with anti-PRAF2 antibodies (Supplementary Figure S6b). A linear correlation was observed between PRAF2 concentration and motor activity, the latter being enhanced even for less than a two-fold increase in PRAF2 concentration. Interestingly, variations in PRAF2 concentration of a comparable or even larger extent are observed in different areas of the brain and different cell types (Figure 1b) and during hippocampal neuron maturation in culture (Supplementary Figure S6c). Together, these data indicate that moderate changes of PRAF2 expression *in vivo* cause significant phenotypic effects.

Correlation between PRAF2-induced hyperactivity and $GABA_B$ function in the VTA

Although consistent with impaired availability of $GABA_B$ sites at the cell surface of VTA neurons, the phenotypic effect of AAV-PRAF2+GFP injection might also be due to the involvement of other receptors or transporters similarly retained by PRAF2 in the ER. To establish a correlation between the observed phenotype and $GABA_B$ function in the VTA, we used several approaches.

Single-cell electrophysiological experiments were performed in dopaminergic neurons of the VTA expressing exogenous PRAF2, to analyse local response to the $GABA_B$ agonist baclofen. AAV-PRAF2+GFP-infected dopaminergic VTA neurons

displayed a markedly impaired current response to baclofen compared to control AAV-GFP-containing neurons, fully consistent with reduced expression of $GABA_B$ at the cell surface (Figures 4c,d,e).

Baclofen stimulation of $GABA_B$ receptors *in vivo* inhibits the enhanced locomotor activity arising from acute stimulation of VTA neurons by amphetamine [53-55]. Consistently, baclofen pretreatment completely inhibited the acute effect of amphetamine in mice bilaterally injected in the VTA with the control virus (Figure 5a). In contrast, although amphetamine administration further enhanced locomotor activity in mice injected with the AAV-PRAF2+GFP virus, baclofen pretreatment failed to abolish this effect, supporting the impairment of $GABA_B$ receptor inhibitory activity in this context (Figure 5b). Interestingly, the VTA-selective bilateral ablation of GB1, achieved by injecting a virus carrying the CRE recombinase (AAV-CRE) in both VTAs of GB1-foxed mice ($GB1^{fl/fl}$), pheno-copied the behavioral effect induced by AAV-PRAF2+GFP in WT mice (Figures 5c and Supplementary Figure S7a). The motor activity of these mice was enhanced by acute administration of amphetamine, but baclofen failed to inhibit the motor effect of amphetamine, similarly to what was observed in wt mice injected with AAV-PRAF2+GFP (compare Figures 5b and 5c).

We next examined the effect of unilateral injection of AAV-PRAF2+GFP virus into the VTA of normal animals or mice displaying global GB1 knock-out [56]. GB1-KO mice exhibit spontaneous hyperlocomotor activity (Figure 5d,e pre-test). Previous studies reported that asymmetric alteration of basal ganglia activity contributes to a rotational behavior [57]; the unilateral increase of dopaminergic activity in the mesolimbic circuit causes contralateral pivoting [58, 59], whereas ipsilateral pivoting is usually associated with reduced activity in the same path [60]. After unilateral injection of AAV-PRAF2+GFP virus into the VTA, leading to a two-fold local increase of

PRAF2 (Supplementary Figure S7b,c), normal control littermates of the GB1-KO mice showed both a significant increase of their overall locomotor activity (Figure 5d,e) and a contralateral turning phenotype (Figure 5f, Movie S1a) compared to control AAV-GFP-injected mice (Movie S1b), confirming that dopaminergic neurons were over-activated in the injected VTA. In contrast, consistent with a functional link between the effect of PRAF2 overexpression and impaired GB1 expression, the unilateral AAV-PRAF2+GFP injection in the VTA of GB1-KO mice neither increased overall activity (Figure 5d,e) nor affected the spontaneous turning phenotype, which was equally contralateral or ipsilateral (Figure 5f). Interestingly, the unilateral deletion of GB1 in the VTA of $GB1^{fl/fl}$ mice (Supplementary Figure S7a) recapitulated the hyperlocomotor activity and the contralateral turning phenotype observed in wt mice receiving unilateral injection of AAV-PRAF2+GFP in the VTA (Figure 5d-f). Together, these data fully support the hypothesis that the behavioral changes induced by modulating the content of PRAF2 in the VTA depend on local $GABA_B$ function.

In conclusion, moderate changes of PRAF2 concentration are sufficient to markedly affect cell surface GB1 targeting and, consequently, $GABA_B$ function both *in vitro* and *in vivo*, via GB1 retention in the ER.

Discussion

PRAF2 functions as an ER gatekeeper that prevents GB1 from egressing the ER until it is competitively displaced by GB2. Thereafter, the GB1-GB2 hetero-dimer can progress to the Golgi apparatus and subsequently to the plasma membrane as a functional $GABA_B$ receptor.

The identification of PRAF2 as a reticular GB1 tether uncovers a central piece of a puzzle initiated by the discovery that $GABA_B$ receptors are hetero-dimers of GB1 and GB2 subunits and that the RXR signal, contained in the carboxy-terminal tail of GB1, participates in GB1 ER retention. A simple mechanism of control of receptor function also emerges from our data, which does not rely on gene transcription or enzymatic protein modification, but rather on the competition between a gatekeeper (PRAF2) and GB2 for interaction with GB1. The fact that cell surface GB1 is dependent on the relative concentrations of competing proteins with opposite effects on its forward trafficking might also explain how functional (although leading to atypical outputs) cell surface GB1 is found in some brain areas of GB2-KO mice [61]. PRAF2 might be less abundant in these particular areas and thus insufficient for retaining all GB1 molecules, which could then reach the cell surface as monomers or homo-dimers. Alternatively, in the absence of GB2, GB1 could hetero-dimerize with another ER-resident GPCR and escape PRAF2 retention.

The concentration of PRAF2 in brain areas is likely submitted to regulation, as, for example, PRAF2 concentration can vary up to 20-fold in embryonic hippocampal neurons after a few days in culture. On the other hand, less than twofold changes in the VTA are sufficient to promote major motor hyperactivity. The mechanistic role of impaired GB1 expression at the surface of VTA neurons in our hyperactive mice was substantiated by several experimental lines of evidence: i) the loss of baclofen-

mediated inhibition of the motor effects caused by amphetamine both in wt mice expressing exogenous PRAF2 in the VTA and mice with localized deletion of GB1 in the VTA; ii) the absence of specific PRAF2 effect in GB1-KO mice; iii) the impaired functional response to baclofen in VTA neurons expressing exogenous PRAF2. It is also consistent with the observation that GB1- or GB2-KO mice exhibit enhanced hyperlocomotor activity [56, 61-63], and that $GABA_B$ antagonists stimulate [64], whereas intra-VTA agonists depress basal locomotor activity [65].

PRAF2 belongs to the short list of specific ER-resident proteins that inhibit the forward export of plasma membrane proteins. These include, Rer1p, which negatively regulates gamma-secretase complex assembly [66], and Shisa a GPCR-interacting, ER-resident protein controlling the surface density of Frizzled during development [18]. Among the other PRAFs, PRAF3, which was reported to somehow control the cell surface function of the Excitatory Amino-Acid Carrier 1 [38, 39], might similarly function as an ER gatekeeper for this protein. So far, although not excluded, there is no experimental evidence that PRAF1 might be a Golgi gatekeeper.

Whereas $GABA_B$ is the only GPCR so far with an identified ER gatekeeper, experimental data suggest that additional members of this receptor family might be controlled by an analogous mechanism. Indeed, either the existence of abundant stores in the ER of primary cells, or regulated delivery to the cell surface were reported for several other GPCRs [6]. In most cases, their association with private chaperones or with escort proteins promoted exit from the ER [7, 12, 67, 68]. In the context of GPCR export in neurons, a depression-like phenotype was observed in knockout mice for p11 [14] a member of the S100 EF-hand calcium-dependent signaling modulators [69], which specifically interacts with serotonin 5-HT_{1B} receptors

(5-HT_{1B}Rs). Cell surface density and function of 5-HT_{1B}Rs were decreased in these mice, indicating that p11 is an escort for 5-HT_{1B}Rs. Interestingly, adenovirus–mediated transfer of the gene encoding p11 to the nucleus accumbens rescued the depression-related behavioral disorders of p11 knockout mice [70]. In light of the data reported here, it is plausible that gatekeepers regulate at least some of these GPCRs in a similar fashion to GB1.

Clinical implications of impaired GPCR export from internal compartments to the cell surface have been documented for several diseases and receptors [71, 72]. In most cases the mechanism of retention was attributed to receptor mutations. Based on our study in mice, a pathological deregulation of gatekeeper content could represent an additional mechanism in this context. Consistent with this hypothesis, a two-threefold increase of *PRAF2* mRNA was reported in human brain tumors compared to normal samples [36, 42].

In conclusion, we have uncovered a mechanism by which GPCR function can be regulated by the competing effects exerted by gatekeepers and escorts on receptor trafficking to the cell surface. Although interfering with this process causes major pathological effects in mice models, further studies are necessary to appreciate whether deregulation of gatekeeper and/or escort expression levels are pathogenic in human diseases.

Acknowledgements

We thank Drs M. Scott (Institut Cochin), M. Bouvier (Université de Montréal, Canada) and J. Epelbaum (Centre de Psychiatrie et Neurosciences, Paris) for their comments; Dr L. Maroteaux (Institut du Fer à Moulin, Paris) for hosting studies in mice; Dr C. Labbé-Jullié (Institut Cochin) for preliminary studies; Dr E. Tzavara (Unité de

Physiopathologie des Maladies du Système Nerveux, Paris) for helpful discussions; the Cochin Institute imaging facility for technical support. This work was supported by grants from the Ligue Contre le Cancer, comité de l'Oise to SD; from the French Agency for AIDS Research (ANRS-09) and the Fondation pour la Recherche Médicale (Equipe FRM-2012) to SM; from the Ecole de Neuroscience de Paris and the INSERM ATIP-Avenir to MM. The authors declare that there are no conflicts of interest. SM team is member of the "Who-am-I" research consortium.

References

1. Doherty GJ, McMahon HT. Mechanisms of Endocytosis. *Annu Rev Biochem* 2009; **78:** 31.31–31.46.

2. Aridor M, Hannan LA. Traffic Jams II: An Update of Diseases of Intracellular Transport. *Traffic* 2002; **3:** 781-790.

3. Hein L, Ishii K, Coughlin SR, Kobilka BK. Intracellular targeting and trafficking of thrombin receptors. A novel mechanism for resensitization of a G protein-coupled receptor. *J Biol Chem* 1994; **269:** 27719-27726.

4. Brismar H, Asghar M, Carey RM, Greengard P, Aperia A. Dopamine-induced recruitment of dopamine D1 receptors to the plasma membrane. *Proc Natl Acad Sci U S A* 1998; **95:** 5573-5578.

5. Saito H, Kubota M, Roberts RW, Chi Q, Matsunami H. RTP family members induce functional expression of mammalian odorant receptors. *Cell* 2004; **119:** 679-691.

6. Achour L, Labbe-Juillie C, Scott MGH, Marullo S. An escort for G Protein Coupled Receptors to find their path: implication for regulation of receptor density at the cell surface. *Trends Pharmacol Sci* 2008; **29:** 528-535.

7. Achour L, Scott MG, Shirvani H, Thuret A, Bismuth G, Labbe-Jullie C *et al.* CD4 - CCR5 interaction in intracellular compartments contributes to receptor expression at the cell surface. *Blood* 2009; **113:** 1938-1947.

8. Holtback U, Brismar H, DiBona GF, Fu M, Greengard P, Aperia A. Receptor recruitment: a mechanism for interactions between G protein-coupled receptors. *Proc Natl Acad Sci U S A* 1999; **96:** 7271-7275.

9. Shirvani H, Achour L, Scott MGH, Thuret A, Bismuth G, Labbe-Juillie C *et al.* Internal stores of CCR5 in blood cells. *Blood* 2011; **118:** 1175-1176.

10. Farhan H, Rabouille C. Signalling to and from the secretory pathway. *J Cell Sci* 2011; **124:** 171-180.

11. Kusek J, Yang Q, Witek M, Gruber CW, Nanoff C, Freissmuth M. Chaperoning of the A1-adenosine receptor by endogenous adenosine - an extension of the retaliatory metabolite concept. *Mol Pharmacol* 2015; **87:** 39-51.

12. McLatchie LM, Fraser NJ, Main MJ, Wise A, Brown J, Thompson N *et al.* RAMPs regulate the transport and ligand specificity of the calcitonin- receptor-like receptor. *Nature* 1998; **393:** 333-339.

13. Bermak JC, Li M, Bullock C, Zhou QY. Regulation of transport of the dopamine D1 receptor by a new membrane- associated ER protein. *Nat Cell Biol* 2001; **3:** 492-498.

14. Svenningsson P, Chergui K, Rachleff I, Flajolet M, Zhang X, El Yacoubi M *et al.* Alterations in 5-HT1B receptor function by p11 in depression-like states. *Science* 2006; **311:** 77-80.

15. Bergmayr C, Thurner P, Keuerleber S, Kudlacek O, Nanoff C, Freissmuth M *et al.* Recruitment of a cytoplasmic chaperone relay by the A2A adenosine receptor. *J Biol Chem* 2013; **288:** 28831-28844.

16. Brock C, Boudier L, Maurel D, Blahos J, Pin JP. Assembly-dependent surface targeting of the heterodimeric GABAB Receptor is controlled by COPI but not 14-3-3. *Mol Biol Cell* 2005; **16:** 5572-5578.

17. Cunningham M, McIntosh K, Pediani JD, Robben J, Cooke AE, Nilsson M *et al.* Novel role for proteinase-activated receptor 2 (PAR2) in membrane trafficking of proteinase-activated receptor 4 (PAR4). *J Biol Chem* 2012; **287:** 16656-16669.

18. Yamamoto A, Nagano T, Takehara S, Hibi M, Aizawa S. Shisa promotes head formation through the inhibition of receptor protein maturation for the caudalizing factors, Wnt and FGF. *Cell* 2005; **120:** 223-235.

19. Benke D. Mechanisms of GABAB receptor exocytosis, endocytosis, and degradation. *Advances in Pharmacology* 2010; **58:** 93-111.

20. Jones KA, Borowsky B, Tamm JA, Craig DA, Durkin MM, Dai M *et al.* GABA(B) receptors function as a heteromeric assembly of the subunits GABA(B)R1 and GABA(B)R2. *Nature* 1998; **396:** 674-679.

21. Kaupmann K, Malitschek B, Schuler V, Heid J, Froestl W, Beck P *et al.* GABA(B)-receptor subtypes assemble into functional heteromeric complexes. *Nature* 1998; **396:** 683-687.

22. White JH, Wise A, Main MJ, Green A, Fraser NJ, Disney GH *et al.* Heterodimerization is required for the formation of a functional GABA(B) receptor. *Nature* 1998; **396:** 679-682.

23. Vigot R, Barbieri S, Bräuner-Osborne H, Turecek R, Shigemoto R, Zhang YP *et al.* Differential compartmentalization and distinct functions of GABAB receptor variants. *Neuron* 2006; **50:** 589-601.

24. Couve A, Filippov AK, Connolly CN, Bettler B, Brown DA, Moss SJ. Intracellular retention of recombinant GABAB receptors. *J Biol Chem* 1998; **273:** 26361-26367.

25. Margeta-Mitrovic M, Jan YN, Jan LY. A trafficking checkpoint controls GABA(B) receptor heterodimerization. *Neuron* 2000; **27:** 97-106.

26. Pagano A, Rovelli G, Mosbacher J, Lohmann T, Duthey B, Stauffer D *et al.* C-terminal interaction is essential for surface trafficking but not for heteromeric assembly of GABA(b) receptors. *J Neurosci* 2001; **21:** 1189-1202.

27. Restituito S, Couve A, Bawagan H, Jourdain S, Pangalos MN, Calver AR *et al.* Multiple motifs regulate the trafficking of GABA(B) receptors at distinct checkpoints within the secretory pathway. *Mol Cell Neurosci* 2005; **28:** 747-756.

28. Kniazeff J, Galvez T, Labesse G, Pin JP. No ligand binding in the GB2 subunit of the GABA(B) receptor is required for activation and allosteric interaction between the subunits. *J Neurosci* 2002; **22:** 7352-7361.

29. Margeta-Mitrovic M, Jan YN, Jan LY. Function of GB1and GB2 subunits in G protein coupling of GABA(B) receptors. *Proc Natl Acad Sci USA* 2001; **98:** 14649–14654

30. Robbins MJ, Calver AR, Filippov AK, Hirst WD, Russell RB, Wood MD *et al.* GABA(B2) is essential for G-protein coupling of the GABA(B) receptor heterodimer. *J Neurosci* 2001; **21:** 8043-8052.

31. Villemure JF, Adam L, Bevan NJ, Gearing K, Chenier S, Bouvier M. Subcellular distribution of GABA(B) receptor homo- and hetero-dimers. *Biochem J* 2005; **388:** 47-55.

32. Laffray S, Bouali-Benazzouz R, Papon MA, Favereaux A, Jiang Y, Holm T *et al.* Impairment of GABAB receptor dimer by endogenous 14-3-3zeta in chronic pain conditions. *EMBO J* 2012; **31:** 3239-3251.

33. Maier PJ, Zemoura K, Acuna MA, Yevenes GE, Zeilhofer HU, Benke D. Ischemia-like oxygen and glucose deprivation mediates down-regulation of cell surface γ-aminobutyric acidB receptors via the endoplasmic reticulum (ER) stress-Induced transcription factor CCAAT/enhancer-binding protein (C/EBP)-homologous protein (CHOP). *J Biol Chem* 2014; **289:** 12896-12907.

34. Kantamneni S, Holman D, Wilkinson KA, Nishimune A, Henley JM. GISP increases neurotransmitter receptor stability by down-regulating ESCRT-mediated lysosomal degradation. *Neuroscience letters* 2009; **452:** 106-110.

35. Abdul-Ghani M, Gougeon PY, Prosser DC, Da-Silva LF, Ngsee JK. PRA isoforms are targeted to distinct membrane compartments. *J Biol Chem* 2001; **276:** 6225-6233.

36. Fo CS, Coleman CS, Wallick CJ, Vine AL, Bachmann AS. Genomic organization, expression profile, and characterization of the new protein PRA1 domain family, member 2 (PRAF2). *Gene* 2006; **371:** 154-165.

37. Sivars U, Aivazian D, Pfeffer SR. Yip3 catalyses the dissociation of endosomal Rab-GDI complexes. *Nature* 2003; **425:** 856-859.

38. Lin CI, Orlov I, Ruggiero AM, Dykes-Hoberg M, Lee A, Jackson M *et al.* Modulation of the neuronal glutamate transporter EAAC1 by the interacting protein GTRAP3-18. *Nature* 2001; **410:** 84-88.

39. Ruggiero AM, Liu Y, Vidensky S, Maier S, Jung E, Farhan H *et al.* The endoplasmic reticulum exit of glutamate transporter is regulated by the inducible mammalian Yip6b/GTRAP3-18 protein. *J Biol Chem* 2008; **283:** 6175-6183.

40. Schweneker M, Bachmann AS, Moelling K. JM4 is a four-transmembrane protein binding to the CCR5 receptor. *FEBS Lett* 2005; **579:** 1751-1758.

41. Koomoa DL, Go RC, Wester K, Bachmann AS. Expression profile of PRAF2 in the human brain and enrichment in synaptic vesicles. *Neurosci Lett* 2008; **436:** 171-176.

42. Borsics T, Lundberg E, Geerts D, Koomoa DL, Koster J, Wester K *et al.* Subcellular distribution and expression of prenylated Rab acceptor 1 domain

family, member 2 (PRAF2) in malignant glioma: Influence on cell survival and migration. *Cancer Sci* 2010; **101:** 1624-1631.

43. Petaja-Repo UE, Hogue M, Laperriere A, Walker P, Bouvier M. Export from the endoplasmic reticulum represents the limiting step in the maturation and cell surface expression of the human delta opioid receptor. *J Biol Chem* 2000; **275:** 13727-13736.

44. Galvez T, Duthey B, Kniazeff J, Blahos J, Rovelli G, Bettler B *et al.* Allosteric interactions between GB1 and GB2 subunits are required for optimal GABA(B) receptor function. *EMBO J* 2001; **20:** 2152-2159.

45. Marullo S, Bouvier M. Resonance Energy Transfer approaches in Molecular Pharmacology and beyond. *Trends Pharmacol Sci* 2007; **28:** 362-365.

46. Achour L, Kamal M, Jockers R, Marullo S. Using quantitative BRET to assess G protein-coupled receptor homo- and heterodimerization. *Methods Mol Biol* 2011; **756:** 183-200.

47. Pinard A, Seddik R, Bettler B. GABAB receptors: physiological functions and mechanisms of diversity. *Advances in Pharmacology* 2010; **58:** 231-255.

48. Cruz HG, Ivanova T, Lunn ML, Stoffel M, Slesinger PA, Luscher C. Bi-directional effects of GABA(B) receptor agonists on the mesolimbic dopamine system. *Nat Neurosci* 2004; **7:** 153-159.

49. Koob GF, Swerdlow NR. The functional output of the mesolimbic dopamine system. *Ann N Y Acad Sci* 1988; **537:** 216-227.

50. Labouebe G, Lomazzi M, Cruz HG, Creton C, Lujan R, Li M *et al.* RGS2 modulates coupling between GABAB receptors and GIRK channels in dopamine neurons of the ventral tegmental area. *Nat Neurosci* 2007; **10:** 1559-1568.

51. Erhardt S, Mathe JM, Chergui K, Engberg G, Svensson TH. GABA(B) receptor-mediated modulation of the firing pattern of ventral tegmental area dopamine neurons in vivo. *Naunyn Schmiedebergs Arch Pharmacol* 2002; **365:** 173-180.

52. Smolders I, De Klippel N, Sarre S, Ebinger G, Michotte Y. Tonic GABA-ergic modulation of striatal dopamine release studied by in vivo microdialysis in the freely moving rat. *Eur J Physiol* 1995; **284:** 83-91.

53. Bartoletti M, Gubellini C, Ricci F, Gaiardi M. The GABAB agonist baclofen blocks the expression of sensitisation to the locomotor stimulant effect of amphetamine. *Behav Pharmacol* 2004; **15:** 397-401.

54. Bartoletti M, Gubellini C, Ricci F, Gaiardi M. Baclofen blocks the development of sensitization to the locomotor stimulant effect of amphetamine. *Behav Pharmacol* 2005; **16:** 553-558.

55. Zhou W, Mailloux AW, McGinty JF. Intracerebral baclofen administration decreases amphetamine-induced behavior and neuropeptide gene expression in the striatum. *Neuropsychopharmacology* 2005; **30:** 880-890.

56. Schuler V, Luscher C, Blanchet C, Klix N, Sansig G, Klebs K *et al.* Epilepsy, hyperalgesia, impaired memory, and loss of pre- and postsynaptic GABA(B) responses in mice lacking GABA(B(1)). *Neuron* 2001; **31:** 47-58.

57. Pycock CJ. Turning behaviour in animals. *Neuroscience* 1980; **5:** 461-514.

58. Koshikawa N. Role of the nucleus accumbens and the striatum in the production of turning behaviour in intact rats. *Rev Neurosci* 1994; **5:** 331-346.

59. Kitamura M, Koshikawa N, Yoneshige N, Cools AR. Behavioural and neurochemical effects of cholinergic and dopaminergic agonists administered into the accumbal core and shell in rats. *Neuropharmacology* 1999; **38:** 1397-1407.

60. Schwarting RK, Huston JP. Unilateral 6-hydroxydopamine lesions of meso-striatal dopamine neurons and their physiological sequelae. *Prog Neurobiol* 1996; **49:** 215-266.

61. Gassmann M, Shaban H, Vigot R, Sansig G, Haller C, Barbieri S *et al.* Redistribution of GABAB(1) protein and atypical GABAB responses in GABAB(2)-deficient mice. *J Neurosci* 2004; **24:** 6086-6097.

62. Vacher CM, Gassmann M, Desrayaud S, Challet E, Bradaia A, Hoyer D *et al.* Hyperdopaminergia and altered locomotor activity in GABAB1-deficient mice. *J Neurochem* 2006; **97:** 979-991.

63. Mombereau C, Kaupmann K, Gassmann M, Bettler B, van der Putten H, Cryan JF. Altered anxiety and depression-related behavior in mice lacking GABAB(2) receptor subunits. . *Neuroreport* 2005; **16:** 307–310.

64. Colombo G, Melis S, Brunetti G, Serra S, Vacca G, Carai MA *et al.* GABA(B) receptor inhibition causes locomotor stimulation in mice. *Eur J Physiol* 2001; **433:** 101-104.

65. Moore EM, Boehm SL, 2nd. Site-specific microinjection of baclofen into the anterior ventral tegmental area reduces binge-like ethanol intake in male C57BL/6J mice. *Behav Neurosci* 2009; **123:** 555-563.

66. Spasic D, Raemaekers T, Dillen K, Declerck I, Baert V, Serneels L *et al.* Rer1p competes with APH-1 for binding to nicastrin and regulates gamma-secretase complex assembly in the early secretory pathway. *J Cell Biol* 2007; **176:** 629-640.

67. Dwyer ND, Troemel ER, Sengupta P, Bargmann CI. Odorant receptor localization to olfactory cilia is mediated by ODR-4, a novel membrane-associated protein. *Cell* 1998; **93:** 455-466.

68. Metherell LA, Chapple JP, Cooray S, David A, Becker C, Ruschendorf F *et al.* Mutations in MRAP, encoding a new interacting partner of the ACTH receptor, cause familial glucocorticoid deficiency type 2. *Nat Genet* 2005; **37:** 166-170.

69. Donato R. Functional roles of S100 proteins, calcium-binding proteins of the EF-hand type. *Biochim Biophys Acta* 1999; **1450:** 191-231.

70. Alexander B, Warner-Schmidt J, Eriksson T, Tamminga C, Arango-Llievano M, Ghose S *et al.* Reversal of depressed behaviors in mice by p11 gene therapy in the nucleus accumbens. *Sci Transl Med* 2010; **2:** 54ra76.

71. Conn PM, Ulloa-Aguirre A, Ito J, Janovick JA. G protein-coupled receptor trafficking in health and disease: lessons learned to prepare for therapeutic mutant rescue in vivo. *Pharmacol Rev* 2007; **59:** 225-250.

72. Valenzano KJ, Benjamin ER, René P, Bouvier M. Pharmacological Chaperons: Potential for the Treatment of Hereditary diseases caused by Mutations in G Protein-Coupled Receptors. In: Gilchrist A (ed). *GPCR Molecular pharmacology and Drug targeting: Shifting Paradigms and New Directions*. Wiley 2010, pp 460-491.

Figure legends

Figure 1. Interaction of PRAF2 and GB1.

(**a**) HEK-293 cells were transfected with plasmids coding for GB1-GFP and/or V5-epitope tagged PRAF2 or PRAF3, as indicated. Immunoprecipitation with a monoclonal anti-V5 antibody was performed from 1mg protein of cell lysates. The presence of GB1 and PRAFs was revealed with anti-GFP and anti-V5 antibodies, respectively. 50 µg of the inputs were analyzed to determine GB1-GFP expression. Lower panel: densitometric analysis of GFP immunoreactivity, corresponding to the GB1-GFP that was co- immunoprecipitated with PRAF-V5 upon incubation with the V5 antibody; AU: arbitrary units; Unpaired t-test **** $p<0.0001$ (N=3). (**b**) PRAF2 and GB1 expression in human (Hela, LN229, U87, U373, THP-1) and mouse cell lines, rat brain, neurons and astrocytes. Immunoblot experiments with Anti-PRAF2 and Anti-GB1 antibodies (see Supplementary Figure S3a for monoclonal anti-GB1 antibody specificity) were conducted on 50µg of total proteins after cell lysis. M: monomeric PRAF2; D: dimeric PRAF2; H: high molecular weight forms likely corresponding to PRAF2 multimers. PRAF2 is also expressed in HEK-293 cells (not shown). (**c**) Coimmunoprecipitation study of endogenous GB1 and PRAF2 from adult rat brains. Experiments were performed on 12mg solubilized brain proteins obtained as described in methods. Samples were immunoprecipitated with control IgG or anti-PRAF2 antibodies, separated by SDS-PAGE and immunoblotted with anti-GB1 or anti-PRAF2 antibodies. 50µg input was co-migrated for comparison. (**d**) Subcellular distribution of PRAF2 and GB1 in rat hippocampal neurons in culture. Permeabilized cells were stained with anti-PRAF2 and anti-GB1 antibodies and antibodies directed against KDEL, to label the ER, or the Golgi marker GM130, then incubated with the

appropriate secondary antibodies coupled to green or red fluochromes. Co-localization (orange in merge panels) was quantified using Image J software. PRAF2 mostly overlapped with KDEL staining (76.7%±6.7%) and a minor fraction overlapped with GM130 staining (8.88±1.1%) in 3 independent experiments; PRAF2 and GB1 overlap was 80,2±5,6%; GB1 and KDEL overlap was 79.7±2.5%. Scale bar: 10 µm. Insets: enlarged areas.

Figure 2. PRAF2 modulation affects cell surface GB1 expression and function in neurons.

(**a**) Hippocampal neurons in culture for 7 days were transfected with control-scrambled or PRAF2-specific siRNAs (Si1 and Si2). After one week, the efficacy of PRAF2 gene silencing was determined by immunoblot experiments on 50µg of total cell lysates using anti-PRAF2 antibodies (see Supplementary Figure S2a). Residual PRAF2 after specific siRNA treatment was compared to values in neurons treated with control siRNA (yellow boxes, n=12). Determination of GB1 binding sites at the surface of siRNA-treated neurons was performed by a radioligand assay, using the hydrophilic GB1-specific (see Supplementary Figure S3c) antagonist [^{3}H]CGP54626 as ligand. One week after transfection, neurons (60-90 x 10^3 per well) were incubated in culture wells with 20 nM [^{3}H]CGP54626 for 20 min at RT, in the absence or presence (to determine non-specific binding) of 10 µM unlabeled CGP54626 (see methods). The number of binding sites after specific siRNA treatment was compared to values in neurons treated with control siRNA (red boxes, n=12). One-way ANOVA **p<0.02; ***p<0.001. (**b**) Expression of exogenous PRAF2 in neurons inhibits the cell-surface density of $GABA_B$ binding sites. Neurons infected with an adenovirus allowing the simultaneous expression of PRAF2 and GFP (AAV-PRAF2+GFP). Upper part: transmission and immunofluorescence microscopy images showing

infected neurons in green; lower part: ligand-binding assay in the same neurons performed as in panel (**a**); Unpaired t-test n=3 *p<0,05. (**c**) Basal spontaneous activity recorded in hippocampal neurons infected with AAVs (as indicated) or transfected with siRNAs, before baclofen treatment. (**d**) The inhibition of spontaneous activity caused by 0.2µM baclofen was measured in additional untreated neurons in the absence or presence of the $GABA_B$ antagonist CGP54626 (100 nM), **p<0.01. (**e**) Dose-response curves of baclofen-induced inhibition of spontaneous action potential discharge were established in untreated neurons, neurons transfected with control siRNA or with PRAF2-specific siRNAs 1 or 2. Data were normalized to neurons under basal conditions and analyzed using GraphPad Prism software, using the one-site inhibition curve as model. The number of recorded neurons for each condition is indicated. Calculated IC_{50} values were: untreated, $7.2x10^{-7}$M (95%CI: $3.0x10^{-7}$-1.710^{-6}); Si-control, $4.5x10^{-7}$M (95%CI: $1.8x10^{-7}$-1.110^{-6}); Si1-PRAF2, $8.0x10^{-8}$M (95%CI: $4.8x10^{-8}$-1.410^{-7}); Si2-PRAF2, $1.3x10^{-7}$M (95%CI: $8.3x10^{-8}$-2.210^{7}). Differences between the various conditions were also analyzed for each concentration of baclofen in the Table S1. (**f**) Comparison of the inhibitory effect of 0.2µM baclofen in untreated neurons, Si-control or Si(1+2)-PRAF2-treated neurons, and neurons infected with AAV-PRAF2+GFP. (**** p<0.0001, untreated versus Si(1+2)-PRAF2; *p<0.05, untreated versus AAV-PRAF2+GFP; Student T-test). For sample current recordings see Supplementary Figure S2b.

Figure 3. Surface GB1 is regulated by PRAF2 and GB2 expression level.

(**a**) HEK-293 cells were transiently cotransfected with the indicated constant amount of myc-GB1-YFP and HA-GB2 plasmid DNA and increasing concentrations of

PRAF2 construct. Surface GB1 in YFP-positive, non-permeabilized cells was quantified by FACS analysis using the 9E10 anti-Myc monoclonal primary antibody and a secondary anti-mouse Cy5-conjugated antibody (Supplementary Figure S4). Cell surface GB1 expression is shown by the histograms: bars indicate SEM from three experiments in duplicate. The amount of the indicated proteins is shown by the immunoblots below the histograms. (**b-d**) GB2 competes with PRAF2 for GB1 interaction. (**b**) Competition between PRAF2 and GB2 for interaction with GB1 in co-IP experiments. HEK-293 cells were transfected with the indicated plasmids. Immunoprecipitation with a monoclonal anti-V5 antibody was performed from 1mg protein of cell lysates. The presence of GB1, GB2 and PRAFs was revealed with anti-GFP, anti-HA and anti-V5 antibodies, respectively. 50 µg of the inputs were analyzed by immunoblot to determine the expression level of the proteins. Lower histograms: densitometric analysis of GFP immunoreactivity, corresponding to the GB1-GFP that was co-immunoprecipitated with PRAF-V5 in the presence of increasing amounts of GB2. *p<0.01 ***p<0.001, one-way ANOVA (n=3). (**c**) BRET saturation experiments of PRAF2-Rluc donor with GB1-YFP acceptor were conducted in the absence or presence of two different amounts of unlabeled GB2 (50ng or 250ng plasmid DNA). Calculated $BRET_{50}$ values were: 1.4±0.3 (GB2=0) 4.9±1.1 (GB2=50) and 12.4±2.5 (GB2=250); n=22 to 66 independent transfections per plot (significant difference between GB2=0 and GB2=250 ($p<0.01$), and between GB2=50 and GB2=250 ($p<0.05$), one-way ANOVA). (**d**) HEK-293 cells were co-transfected with the constant amounts of myc-GB1-YFP and PRAF2-V5 plasmids and increasing concentrations of HA-GB2 plasmid. Cell surface export of GB1 was examined by FACS on non-permeabilized cells, as described in panel a. (**e**) Involvement of the GB1 RXR and LL motifs in the interaction with PRAF2. Co-

immunoprecipitation experiments conducted as in Figure 1a comparing the association of GB1-GFP, GB1-ASA-GFP, GB1-AA-GFP and GB1-AA/ASA-GFP with PRAF2-V5; bottom: quantitation of immunoprecipitated material. Tub: tubulin loading control; ***p<0.0001 ****p<0.00001, one way Anova, from 4 independent experiments.

Figure 4. Locomotor activity and baclofen-evoked $GABA_B$ currents in mice expressing exogenous PRAF2 in the VTA

(**a**) Locomotor activity and habituation to a novel environment of mice receiving bilateral injection in the VTA of AAV-GFP (open symbols) or AAV-PRAF2+GFP (filled symbols) after 1 (Day 1), 2 (Day 2) or 3 (Day 3) days of habituation. Locomotor activity was measured in a circular corridor with four infrared beams placed every 90°. Counts corresponding to consecutive interruption of two adjacent beams (i.e., mice moving through one-quarter of the corridor) were incremented every 5 min. The effects of 200 or 500 nL of injected virus are shown (n=16 in each group). For open symbols, error bars are smaller than the size of the symbols. See Supplementary Figures S6-7 for quantitative analysis of PRAF2 expression in the VTA. (**b**) Habituation had no effect in AAV-PRAF2+GFP-injected mice (lower panels), whereas AAV-GFP-injected mice (upper panels), showed reduced locomotor activity at days 2 and 3 (D2 and D3) compared to the first day (D1). Data were analyzed using two-way ANOVA (means±SEM) ****P<0.0001 Df(1). (**c-e**) Overexpression of PRAF2 in the VTA reduces baclofen-evoked $GABA_B$ currents. (**c**) Visualization of the injection area of AAV-PRAF2-GFP or control AAV-GFP (left panel) and of transfected neurons (middle panel). Three weeks after injection, GFP-positive VTA neurons were patch-clamped under visual guidance (right panel) to assess baclofen-induced currents.

Scale bar, 20 µm (**d**). Left panel: example of traces of VTA GFP-positive neurons exhibiting *h*-current (left scale bars 200 ms and 100 pA) in response to bath-application of baclofen (15 µM) with an outward current, which was blocked by the $GABA_BR$-antagonist CGP52432 (5 µM) (right scale bars 2min and 50 pA). (**e**) Peak maximal current in putative VTA dopamine neurons infected with either control AAV-GFP (black column), or AAV-PRAF2+GFP (red column). A significant decrease in the maximal baclofen-induced current was observed in neurons expressing exogenous PRAF2 (Control: 220.65±57.24 pA, n=8; AAV-PRAF2+GFP: 74.78±30.38 pA, n=10; t(16)=2.383, *p<0.05). The baclofen-induced current was typically partly desensitized, reaching a steady state current (I steady). Compared to control neurons, VTA dopamine neurons expressing exogenous PRAF2 displayed reduced steady state currents (Control: 156.63±43.32 pA, n=8; AAV-PRA2+GFP: 59.59±19.64 pA, n=10; t(16)=2.189, p<0.05), and also exhibited less desensitization (I max – I steady) currents (Control: 64.03±19.38 pA, n=8; AAV-PRAF2+GFP: 15.19±12.23 pA, n=10; t(16)=2.217, p<0.05).

Figure 5. Behavioral changes induced by modulating the content of PRAF2 in the VTA depend on local $GABA_B$ function.

(**a-c**) Overexpression of PRAF2 in the VTA reduces baclofen dependent behavioral effects. The effect of baclofen (4mg/kg, i.p.) on amphetamine-induced locomotor activity was examined in wt mice (**a, b**) injected bilaterally with 200nL of AAV-GFP (**a**) or AAV-PRAF2+GFP (**b**) (n=8 in each group) or $GB1^{fl/fl}$ mice injected bilaterally with 200nL of AAV-CRE-GFP (**c**) (n=6). Animals received saline (open symbols) or baclofen (filled symbols) 30min before amphetamine (3mg/kg, i.p. squares) or saline (circles) administration. Locomotor activity was then recorded for 2h. Data (means ±

SEM, *n* = 6-8 per group) were analyzed by two-way ANOVA with treatment as main factor (F(5,31)=6,083 P=0,0005), revealing the following significant interactions: AAV-PRAF2+GFP saline+AMPH vs. AAV-GFP baclo+AMPH (p<0.001); AAV-PRAF2+GFP baclo+AMPH vs. AAV-GFP baclo+AMPH (p<0.001); AAV-GFP saline+AMPH vs. AAV-GFP baclo+AMPH (p<0.01). AAV-GFP baclo+AMPH vs. AAV-CRE saline+AMPH (P<0.001); AAV-GFP baclo+AMPH vs. AAV-CRE baclo+AMPH (p<0.001). No interaction was found for: AAV-PRAF2+GFP saline+AMPH vs. AAV-PRAF2+GFP baclo+AMPH; AAV-PRAF2+GFP saline+AMPH vs. AAV-GFP saline+AMPH; AAV-PRAF2+GFP baclo+AMPH vs. AAV-GFP saline+AMPH; AAV-CRE saline+AMPH vs. AAV-CRE baclo+AMPH; AAV-GFP saline+AMPH vs. AAV-CRE baclo+AMPH; AAV-GFP saline+AMPH vs. AAV-CRE saline+AMPH. Arrows indicate amphetamine/saline injection. (**d-f**) Loss of PRAF2-dependent behavioral effects in GB1-KO mice. The locomotor effect of AAV-PRAF2+GFP unilateral injection in the VTA of GB1-KO mice and control littermates (WT) was compared with that of AAV-CRE-GFP injection in the VTA of $GB1^{fl/fl}$ mice. Spontaneous locomotor activity of each mouse was measured two weeks before (Pre-test) or after (Test) unilateral injection of AAV-PRAF2+GFP or AAV-CRE-GFP in the VTA. In WT mice, PRAF2 induced a significant homogeneous enhancement of motor activity (video-tracking in (**d**), quantification in (**e**) one-way ANOVA p=0,001; n=10). In GB1-KO mice Pre-test locomotor activity was enhanced on average, comparatively to WT animals, one-way ANOVA p=0,0365 (with marked variations between individuals), but was not enhanced by exogenous PRAF2 expression in the VTA, one-way ANOVA p=0,371; n=10. In $GB1^{fl/fl}$ mice CRE induced a significant enhancement of motor activity comparable to that caused by PRAF2 in wt mice, one-way ANOVA p= 0,001. (**f**) Number and direction of turns recorded for WT and GB1-KO mice after

AAV-PRAF2+GFP injection in the VTA and for $GB1^{fl/fl}$ mice after AAV-CRE-GFP injection in the VTA. n.s: non significant.

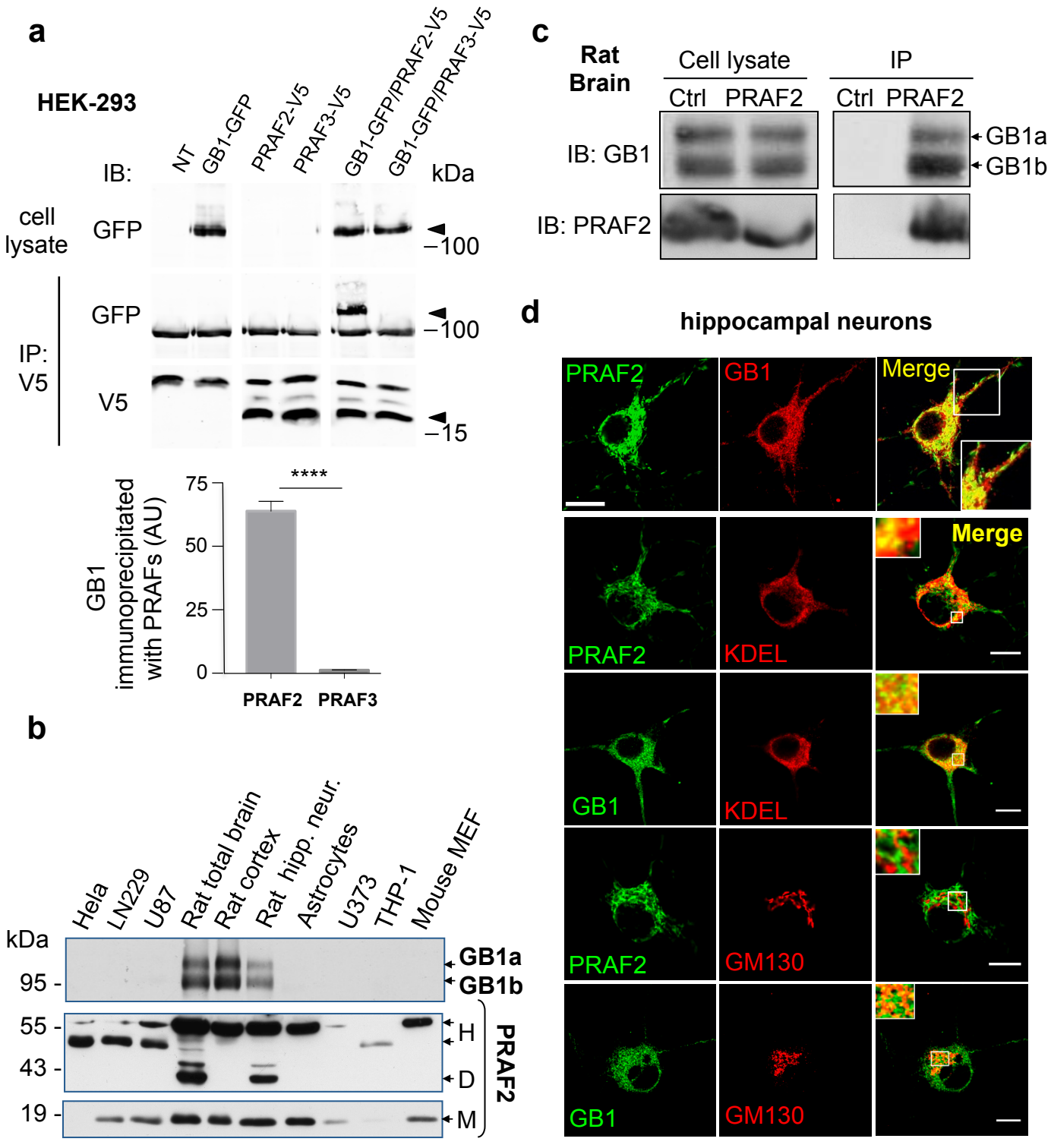
a
HEK-293
NT
GB1-GFP
PRAF2-V5
PRAF3-V5
GB1-GFP/PRAF2-V5
GB1-GFP/PRAF3-V5
IB:
kDa
cell lysate
GFP
100
IP: V5
GFP
100
V5
15
GB1 immunoprecipitated with PRAFs (AU)
****
75
50
25
0
PRAF2
PRAF3
b
Hela
LN229
U87
Rat total brain
Rat cortex
Rat hipp. neur.
Astrocytes
U373
THP-1
Mouse MEF
kDa
95
55
43
19
GB1a
GB1b
H
D
M
PRAF2
c
Rat Brain
Cell lysate
IP
Ctrl
PRAF2
Ctrl
PRAF2
IB: GB1
IB: PRAF2
GB1a
GB1b
d
hippocampal neurons
PRAF2
GB1
Merge
PRAF2
KDEL
Merge
GB1
KDEL
PRAF2
GM130
GB1
GM130

Figure 1

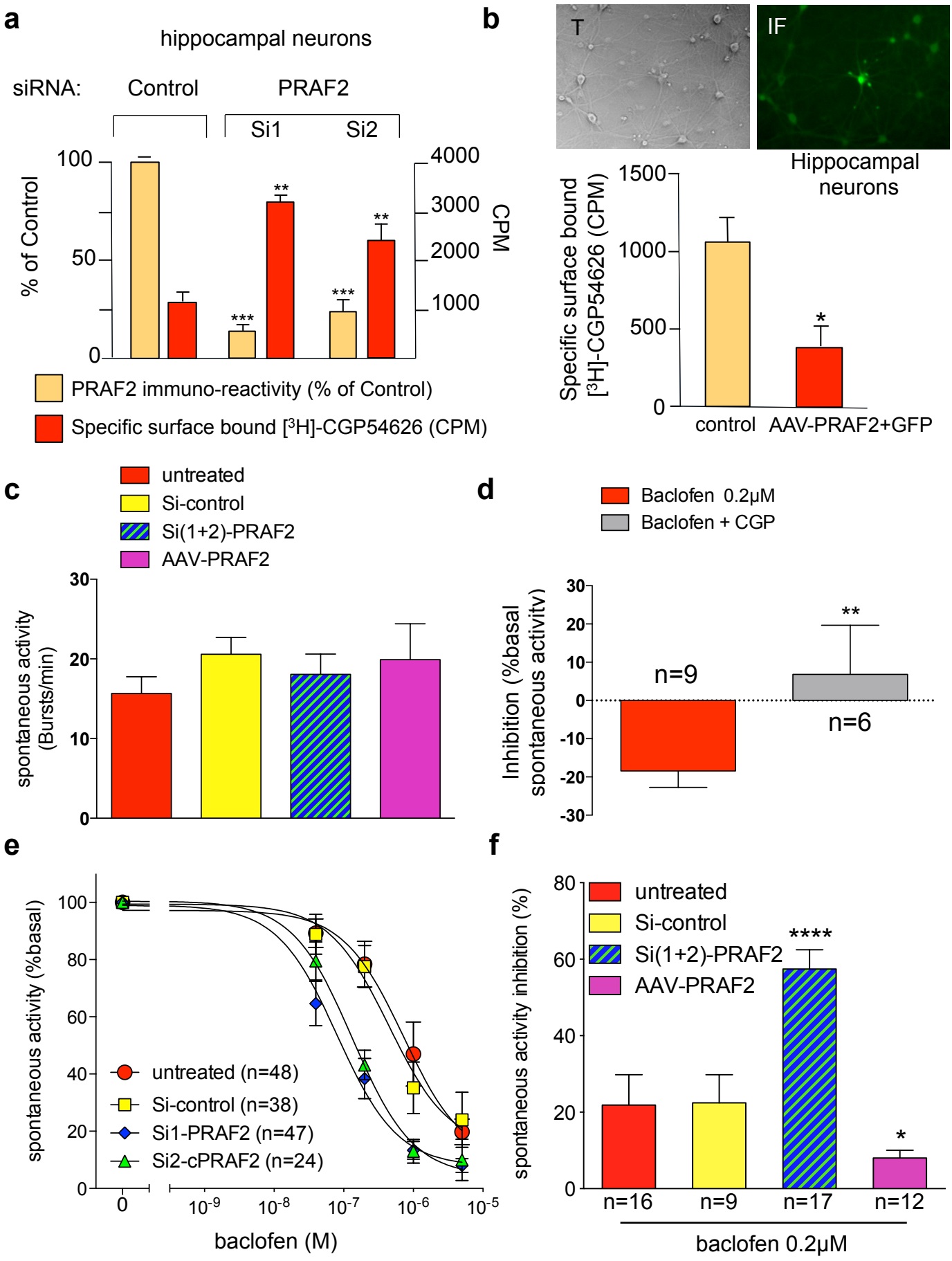
a
hippocampal neurons
siRNA:
Control
PRAF2
Si1
Si2
% of Control
CPM
PRAF2 immuno-reactivity (% of Control)
Specific surface bound [3H]-CGP54626 (CPM)
b
T
IF
Hippocampal neurons
Specific surface bound [3H]-CGP54626 (CPM)
control
AAV-PRAF2+GFP
c
untreated
Si-control
Si(1+2)-PRAF2
AAV-PRAF2
spontaneous activity (Bursts/min)
d
Baclofen 0.2µM
Baclofen + CGP
Inhibition (%basal spontaneous activity)
n=9
n=6
e
spontaneous activity (%basal)
untreated (n=48)
Si-control (n=38)
Si1-PRAF2 (n=47)
Si2-cPRAF2 (n=24)
baclofen (M)
f
spontaneous activity inhibition (%)
untreated
Si-control
Si(1+2)-PRAF2
AAV-PRAF2
n=16
n=9
n=17
n=12
baclofen 0.2µM

Figure 2

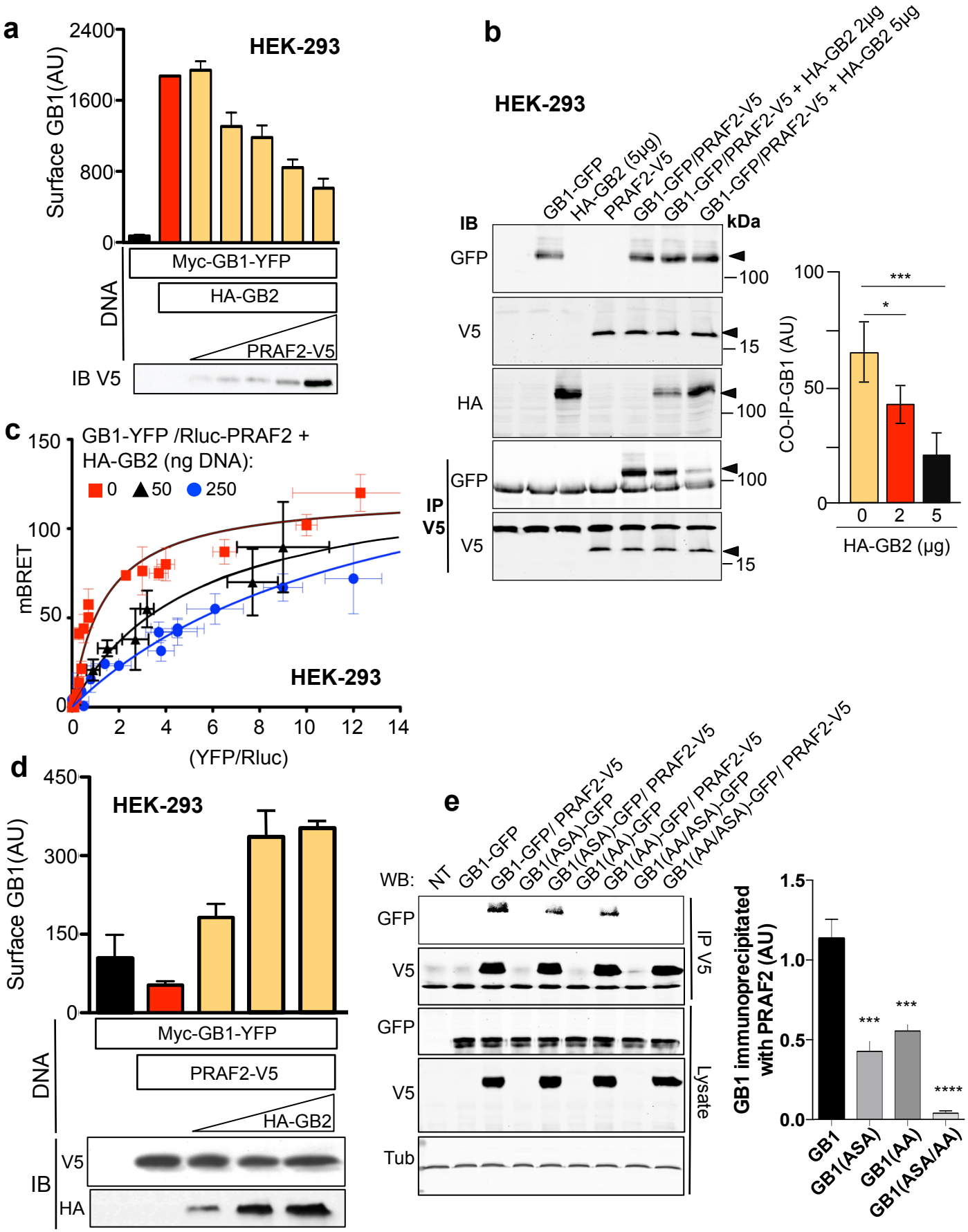
a
HEK-293
Surface GB1(AU)
2400
1600
800
0
DNA
Myc-GB1-YFP
HA-GB2
PRAF2-V5
IB V5
b
HEK-293
GB1-GFP
HA-GB2 (5µg)
PRAF2-V5
GB1-GFP/PRAF2-V5
GB1-GFP/PRAF2-V5 + HA-GB2 2µg
GB1-GFP/PRAF2-V5 + HA-GB2 5µg
IB
kDa
GFP
V5
HA
IP V5
100
15
CO-IP-GB1 (AU)
***
*
HA-GB2 (µg)
c
GB1-YFP /Rluc-PRAF2 +
HA-GB2 (ng DNA):
0
50
250
mBRET
HEK-293
(YFP/Rluc)
d
HEK-293
Surface GB1(AU)
450
300
150
0
Myc-GB1-YFP
PRAF2-V5
HA-GB2
IB
V5
HA
e
WB:
NT
GB1-GFP
GB1-GFP/ PRAF2-V5
GB1(ASA)-GFP
GB1(ASA)-GFP/ PRAF2-V5
GB1(AA)-GFP
GB1(AA)-GFP/ PRAF2-V5
GB1(AA/ASA)-GFP
GB1(AA/ASA)-GFP/ PRAF2-V5
GFP
V5
Tub
IP V5
Lysate
GB1 immunoprecipitated with PRAF2 (AU)
1.5
1.0
0.5
0.0
***
***
****
GB1
GB1(ASA)
GB1(AA)
GB1(ASA/AA)

Figure 3

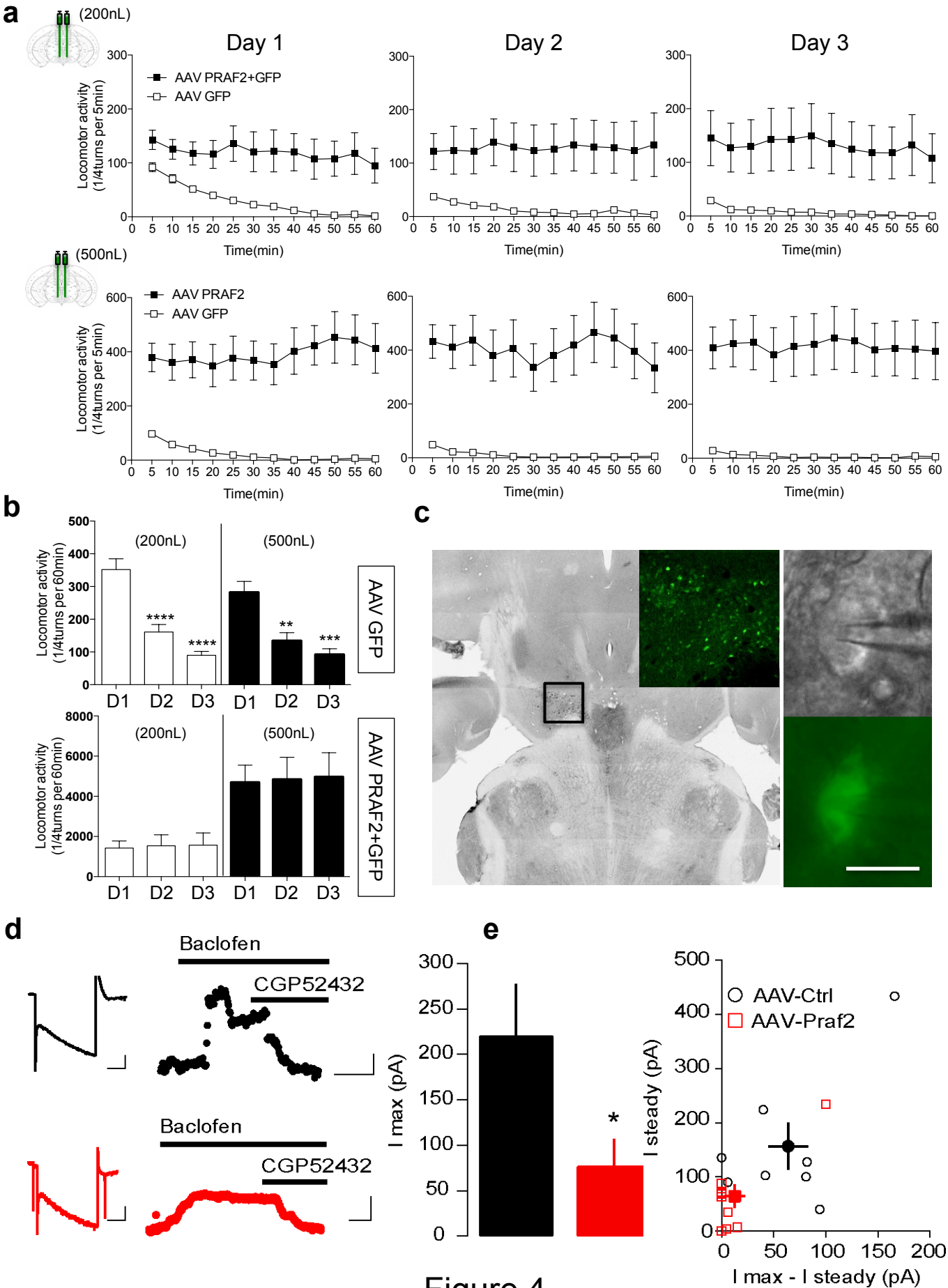
a
(200nL)
Day 1
Day 2
Day 3
AAV PRAF2+GFP
AAV GFP
Locomotor activity (1/4turns per 5min)
Time(min)
(500nL)
AAV PRAF2
AAV GFP
b
(200nL)
(500nL)
Locomotor activity (1/4turns per 60min)
AAV GFP
AAV PRAF2+GFP
D1
D2
D3
c
d
Baclofen
CGP52432
e
I max (pA)
I steady (pA)
AAV-Ctrl
AAV-Praf2
I max - I steady (pA)

Figure 4

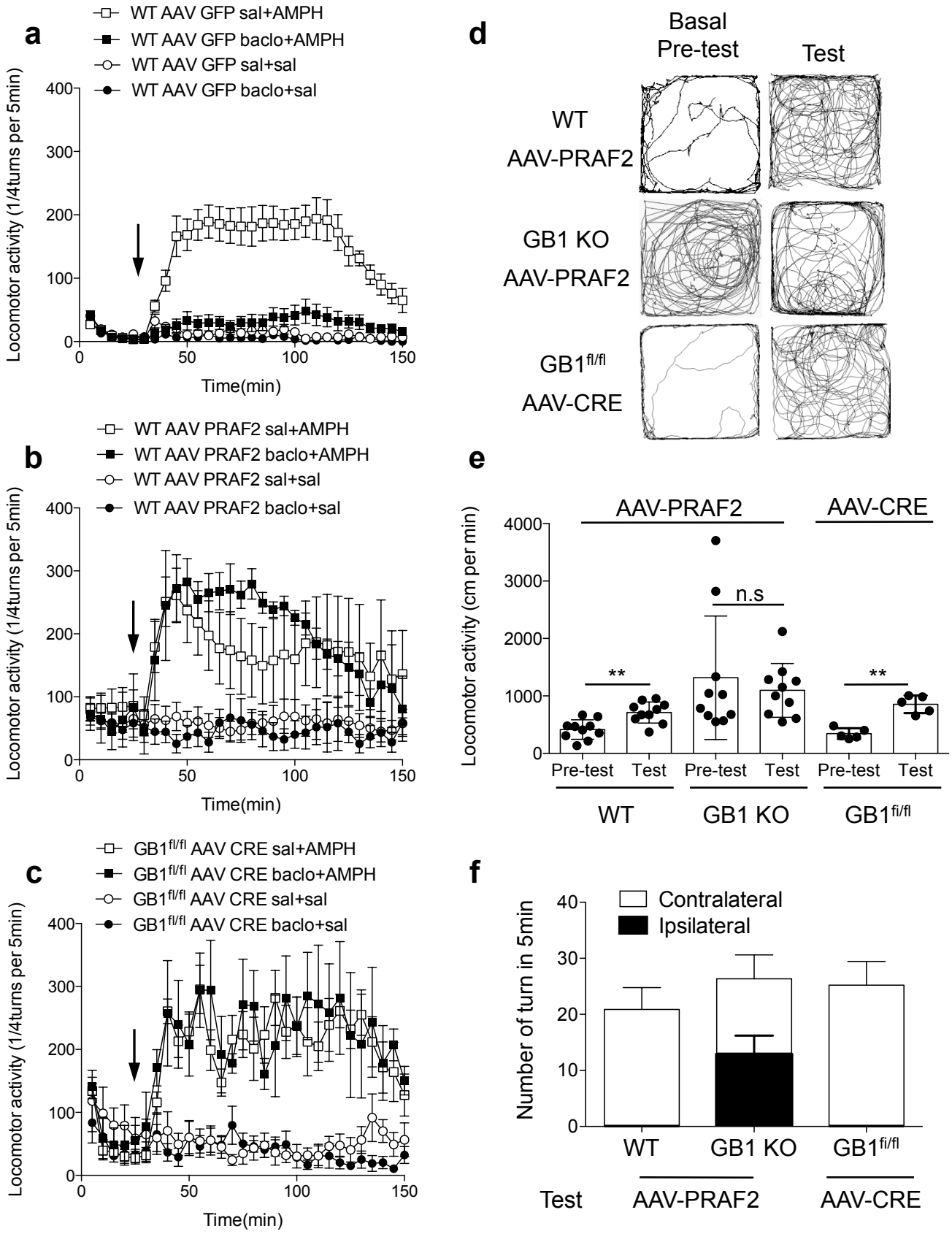
a
WT AAV GFP sal+AMPH
WT AAV GFP baclo+AMPH
WT AAV GFP sal+sal
WT AAV GFP baclo+sal
Locomotor activity (1/4turns per 5min)
Time(min)
b
WT AAV PRAF2 sal+AMPH
WT AAV PRAF2 baclo+AMPH
WT AAV PRAF2 sal+sal
WT AAV PRAF2 baclo+sal
Locomotor activity (1/4turns per 5min)
Time(min)
c
GB1fl/fl AAV CRE sal+AMPH
GB1fl/fl AAV CRE baclo+AMPH
GB1fl/fl AAV CRE sal+sal
GB1fl/fl AAV CRE baclo+sal
Locomotor activity (1/4turns per 5min)
Time(min)
d
Basal
Pre-test
Test
WT
AAV-PRAF2
GB1 KO
AAV-PRAF2
GB1fl/fl
AAV-CRE
e
AAV-PRAF2
AAV-CRE
Locomotor activity (cm per min)
n.s
**
**
Pre-test
Test
Pre-test
Test
Pre-test
Test
WT
GB1 KO
GB1fi/fl
f
Contralateral
Ipsilateral
Number of turn in 5min
WT
GB1 KO
GB1fi/fl
Test
AAV-PRAF2
AAV-CRE

Figure 5

Bonferroni's multiple comparisons test	Mean Diff,	95% CI of diff,	Summary	N1	N2	t	DF
Baclofen 0µM							
untreated vs. Si-control	0	-19,56 to 19,56	ns	12	9	0	137
untreated vs. Si1-PRAF2	0	-18,11 to 18,11	ns	12	12	0	137
untreated vs. Si2-cPRAF2	0	-22,18 to 22,18	ns	12	6	0	137
Si-control vs. Si1-PRAF2	0	-19,56 to 19,56	ns	9	12	0	137
Si-control vs. Si2-cPRAF2	0	-23,38 to 23,38	ns	9	6	0	137
Si1-PRAF2 vs. Si2-cPRAF2	0	-22,18 to 22,18	ns	12	6	0	137
Baclofen 0.04µM							
untreated vs. Si-control	0,3929	-20,70 to 21,49	ns	12	7	0,04986	137
untreated vs. Si1-PRAF2	24,63	4,381 to 44,87	**	12	8	3,256	137
untreated vs. Si2-cPRAF2	9,75	-15,86 to 35,36	ns	12	4	1,019	137
Si-control vs. Si1-PRAF2	24,23	1,277 to 47,19	*	7	8	2,826	137
Si-control vs. Si2-cPRAF2	9,357	-18,44 to 37,16	ns	7	4	0,9011	137
Si1-PRAF2 vs. Si2-cPRAF2	-14,88	-42,04 to 12,29	ns	8	4	1,466	137
Baclofen 0.2µM							
untreated vs. Si-control	0,873	-21,48 to 23,22	ns	7	9	0,1046	137
untreated vs. Si1-PRAF2	40,03	18,17 to 61,89	****	7	10	4,903	137
untreated vs. Si2-cPRAF2	35,26	10,59 to 59,94	**	7	6	3,826	137
Si-control vs. Si1-PRAF2	39,16	18,78 to 59,53	****	9	10	5,144	137
Si-control vs. Si2-cPRAF2	34,39	11,01 to 57,76	***	9	6	3,938	137
Si1-PRAF2 vs. Si2-cPRAF2	-4,767	-27,67 to 18,14	ns	10	6	0,5572	137
Baclofen 1µM							
untreated vs. Si-control	11,86	-11,10 to 34,81	ns	8	7	1,383	137
untreated vs. Si1-PRAF2	33,67	13,42 to 53,91	***	8	12	4,452	137
untreated vs. Si2-cPRAF2	34	8,715 to 59,29	**	8	5	3,6	137
Si-control vs. Si1-PRAF2	21,81	0,7155 to 42,90	*	7	12	2,768	137
Si-control vs. Si2-cPRAF2	22,14	-3,828 to 48,11	ns	7	5	2,283	137
Si1-PRAF2 vs. Si2-cPRAF2	0,3333	-23,28 to 23,94	ns	12	5	0,0378	137
Baclofen 5µM							
untreated vs. Si-control	-4,222	-27,60 to 19,15	ns	9	6	0,4835	137
untreated vs. Si1-PRAF2	11,78	-12,96 to 36,52	ns	9	5	1,275	137
untreated vs. Si2-cPRAF2	9,778	-19,79 to 39,35	ns	9	3	0,8853	137
Si-control vs. Si1-PRAF2	16	-10,86 to 42,86	ns	6	5	1,595	137
Si-control vs. Si2-cPRAF2	14	-17,36 to 45,36	ns	6	3	1,195	137
Si1-PRAF2 vs. Si2-cPRAF2	-2	-34,39 to 30,39	ns	5	3	0,1653	137

Table 1. Statistical analysis of values in Figure 2e

Legends to Supplementary Figures

Supplementary Figure S1. PRAF2 interacts with GB1 in the ER but does not modulate GB2 cell surface expression.

(**a**) PRAF2 selectively interacts with GB1 (b isoform, lower arrowhead) compared to GB2 (upper arrowhead). HEK-293 cells were transfected with the indicated plasmids and processed as in (Figure 1a). Lower panel: densitometric analysis of GB1-GFP or GB2-GFP co-immunoprecipitated with PRAF2; Unpaired t- test *** $p<0.001$ (N=3). (**b**) Glycosylation profile of GB1 interacting with PRAF2. HEK-293 cells were transfected with the indicated plasmids. Cell lysates (upper panel, 5% of the input) or material immuno-precipitated with anti-V5 antibodies (as in Figure 1a, lower panel), were incubated overnight at 37°C with buffer alone or buffer containing glycosidases: Endo H (50.000 U/ml, final), cleaves glycans added in the ER, which cannot be cleaved anymore after additional glycosylation occurring in the Golgi apparatus; PNGase (50.000 U/ml, final), cleaves all added N-glycans. In the presence of GB2, minimal amounts of GB1 were deglycosylated by Endo H in the cell lysate, whereas after immuno-precipitation of PRAF2, co-IPd GB1 appeared mostly sensitive to the enzyme. (**c**) Hippocampal neurons infected with the AAV-PRAF2-GFP as in (Figure 2b), or with a control AAV-GFP virus were fixed and stained with the anti-GB2 antibody without permeabilization (see Supplementary Figure S3b for GB2 antibody specificity). Wide-field or confocal IF images (at mid distance between the bottom and the top of the cells for confocal images) were taken. Note that no labeling was observed in these non-permeabilized neurons with an antibody directed against the intracellular C-tail of GB2 (not shown). Lower graph: Quantitation of surface-associated GB2 immunoreactivity in GFP-containing neurons (n=30). AAV-PRAF2-

GFP: 50.0±14.9; AAV-GFP: 50.1±15.8 (NS). Bar 10µm. (**d**) Surface GB2 expression analyzed by FACS in non-permeabilized cells expressing stable amounts of GB2 (measured by FACS analysis on prermeabilized cells, not shown) and increasing amounts of PRAF2-V5.

Supplementary Figure S2. Electrophysiological study in hippocampal neurons

(**a**) Hippocampal neurons in culture for 7 days were transfected with control-scrambled or PRAF2-specific siRNAs (Si1 and Si2). After one week, the efficacy of PRAF2 gene silencing was determined by immunoblot experiments on 50µg of total cell lysates using anti-PRAF2 antibodies. Actin immunoreactivity was used as loading control. (**b**) Sample current clamp recordings of spontaneous action potential discharge in basal conditions, in the presence of 0.2µM baclofen and after washing, from non-transfected neurons (control) or neurons transfected with PRAF2 siRNAs (PRAF2 siRNA). (1-3) Traces are from 3 independent preparations of neurons (control and PRAF2 siRNA comparisons were done on the same preparation).

Supplementary Figure S3. Specificity of antibodies and [3H]-CGP54626 for $GABA_B$ subunits.

Immunofluorescence studies were conducted on HEK-293 cells transfected with the constructs for GB1-GFP or GB2-GFP. (**a**) The GFP-associated fluorescence was compared to the anti-GB1 antibody-associated fluorescence. Arrowheads indicate a non-transfected cell. Cells expressing GB2-GFP and the non-transfected cell were not labeled by the anti-GB1 antibody. (**b**) The GFP-associated fluorescence was compared to the anti-GB2 antibody-associated fluorescence. Cells expressing GB1-GFP were not labeled by the anti-GB2 antibody. (**c**) Competition radioligand binding

assays with [3H]CGP54626 and unlabeled CGP54626 were conducted on membranes (100µg per assay), prepared from GB1-GFP or GB2-GFP transfected HEK-293 cells, expressing equivalent amounts of recombinant receptors. Only background levels of bound [3H]-CGP54626 were measured in membranes from GB2-GFP-expressing cells.

Supplementary Figure S4. Receptor cell-surface export analysis

HEK-293 expressing Myc-GB1-YFP alone or co-expressed with HA-GB2 and/or PRAF2-V5 were processed as described in the "Receptor cell-surface export analysis" section of "Supplementary Experimental Procedures". The Figure shows a representative example of FACS analysis and calculation of surface GB1 in HEK-293 cells expressing Myc-GB1-YFP in the absence or presence of HA-GB2. CY5 and YFP signals correspond to surface and total Myc-GB1-YFP, respectively. Gated cells were distributed in 4 groups: double negative (non-transfected, group 1), YFP-positive and CY5-negative (group 2), YFP- and CY5-double positive (group 3), YFP-negative and CY5-positive (group 4, this last group being routinely close or equal to zero). The total amount of expressed receptor was used for experiment calibration. This value was equivalent (±10%) for all experiments. It was calculated by adding the products of the % of cells expressing YFP multiplied by the mean YFP-associated fluorescence intensity of groups 2 and 3. The amount of surface GB1 corresponded to the % of the cells in group 3 multiplied by the mean CY5 signal of the group, this product corresponding to the arbitrary units indicated in the figures. Thus, in cells expressing Myc-GB1-YFP alone (left panels), total GB1 expression was (59,79% x 40816,73) + (10,72% x 150274,57)= 40482 whereas GB1 surface expression corresponded to 10,72% x 942,27= 100,8 A.U. In cells co-expressing Myc-GB1-YFP

and HA-GB2 (right panels), total GB1 expression was (39,57% x 12069,01) + (33,48% x 108604,78)= 40979, whereas GB1 surface expression corresponded to 33,48% x 5498,88= 1841 A.U.

Supplementary Figure S5. Exogenous PRAF2 and GB2 modulate subcellular distribution of GB1 in HEK-293 cells.

HEK-293 cells were transiently transfected with various combinations of plasmids encoding GB1-GFP, HA-GB2 or PRAF2-V5. Triton-permeabilized cells were labeled with anti-V5 (to detect exogenous PRAF2), anti-HA (to detect exogenous GB2) and primary anti-BIP antibodies, as indicated, and then with the appropriate secondary antibodies before confocal immunofluorescence analysis. Co-localization was determined as in Figure 1. (**a**) In the absence of GB2, 92.9±1.3% (mean ±SEM, n=40) of GB1-GFP and 98,1±0.5% (n=10) of the PRAF2-V5/GB1-GFP co-localized signal overlapped with the anti-BIP signal. (**b, c**) in the presence of exogenous HA-GB2, 95.4±0.9% of GB1-GFP was colocalized with HA-GB2, mostly in the peripheral area of the cells (n=20). (**d, e**) The redistribution of GB1-GFP observed in the presence of HA-GB2 was counteracted by the simultaneous expression of exogenous PRAF2, the GB1-GB2 colocalization dropping to 53.4±3.2% (n=20). Scale bar: 10µM. (**f-h**) Quantitative analysis of GB1 subcellular distribution**.** Confocal images of the cells above (optical magnification: 60x, digital zoom, 1x, resolution: 10 pixels/µm, laser intensity set at 20% of the maximum) were acquired. Quantitative analysis of GF1-GFP distribution was achieved by measuring the fluorescence intensity along an axis passing across each examined cell from one side of the plasma membrane to the other, outside the nuclear area, in the same focal plane of each analyzed cell (dashed line). Fluorescence values (expressed as the % of the

maximal value in the examined field) were plotted pixel by pixel from left to right. n=20 to 40 per condition.

Supplementary Figure S6. Distribution and quantitative analysis of exogenous PRAF2 in the VTA of AAV-PRAF2+GFP injected mice.

(**a**) Imaging of the virus diffusion and characterization of the infected neurons of the VTA. Mice that received bilateral stereotactic injection of 500nL of AAV-PRAF2+GFP virus in the VTA were sacrificed. Coronal sections of the brains were analyzed using Tyrosine Hydroxylase (TH, the rate-limiting enzyme in the synthesis of catecholamines) antibodies (red) to identify dopaminergic VTA neurons. GFP fluorescence revealed the distribution of the AAV-PRAF2+GFP virus, relatively to the targeted VTA. Panels “a” and “b” show higher magnification of the corresponding boxed areas. Overlays were used to appreciate colocalization. Arrowheads, indicate virus-infected dopaminergic neurons, whereas asterisks indicate non-infected dopaminergic neurons. In panels “b” the arrows indicate infected non- dopaminergic neurons. VTA: ventral tegmental area; SNR: substancia nigra reticulata; SNC: substancia nigra compacta; cp: cerebral peduncle. Bars: 200 µm in low-magnification images, 20 µm, in panels “a” and “b”. (**b**) Quantitation of AAV-PRAF2+GFP-induced PRAF2 expression in mouse VTA**.** Locomotor activity of mice that received bilateral injection of either AAV-GFP (# 1,2,3) or AAV-PRAF2+GFP virus (# 4,5,6,7) in the VTA, was recorded during one hour. Mice were then sacrificed and PRAF2 and tubulin expression quantitated by immunoblot analysis of VTA extracts (duplicates). Lower panel: average tubulin-normalized PRAF2 values were plotted against the locomotor activity of each corresponding mouse. r= Pearson correlation coefficient. (**c**) Changes in PRAF2 expression during hippocampal neuron maturation in culture**.**

Hippocampal neurons were lysed after the indicated number of days in culture (DIV) and used for immunoblot analysis of PRAF2 and GB1 expression as in Figure 1. After normalization, densitometric analysis (Image J software) showed that PRAF2 concentration increased progressively up to 20 times form DIV5 and DIV8.

Supplementary Figure S7. Quantitative analysis of GB1 and PRAF2 in the VTA of unilaterally injected mice.

(a) VTA-selective GB1 KO in GB1fl/fl mice. GB1fl/fl mice were unilaterally or bilaterally (not shown) injected with AAV CRE-GFP (coding for CRE recombinase-GFP fusion protein) in the VTA, as shown in the diagram, to locally disrupt GB1 expression. Fluorescence imaging of nuclear CRE-GFP is shown at increasing magnification. The Box corresponds to magnified areas. Right panels: protein extracts from the VTA were analyzed by immunoblot with anti-GB1 antibodies. GB1 expression was reduced in the injected VTA comparatively to the non-injected contralateral region. Densitometric analysis of the specific immunoreactive material was carried on 5 samples. ***p<0.001. (**b, c**) Quantitation of PRAF2 expression in the VTA of mice unilaterally injected with 500nL of AAV-PRAF2+GFP **(b)** Red fluorescence corresponds the anti-PRAF2 antibody labeling; GFP fluorescence shows AAV-PRAF2+GFP distribution in coronal sections. Lower panels correspond to the magnification of the “a” squares; Top and bottom bars: 500 and 30µm, respectively. Asterisks show infected neurons (GFP, and PRAF2-positive), arrowheads show uninfected neurons. Upper histograms: PRAF2-associated fluorescence, normalized over background PRAF2 values in contralateral non-infected neurons. (Mean±SEM of 75 neurons, Unpaired t-test p<0.0001; Lower histograms: expression of the data above as the fold change in infected compared to non-infected neurons (n=75 in each group). (**c**) VTA extracts were processed for

immunoblot experiments with anti-PRAF2 antibodies. Representative immunoblots from 2 mice injected with AAV-GFP in the right VTA and with AAV-PRAF2+GFP in the left VTA. Right histogram: for quantitation of the immunoblots (4 mice, triplicates), the PRAF2 signal was normalized with that of tubulin. Mean density (±SEM) is shown, $p<0.0001$. Data were analyzed using unpaired t-test. As in mice bilaterally injected in the VTA, a 2-3 fold increase of PRAF2 expression was sufficient to induce the phenotypic effects.

Movies

Mice injected unilaterally with the AAV-PRAF2+GFP virus or the control AAV-GFP virus

(**Movie S1a**) Video file of mice unilaterally injected in the right VTA with 500 nL of AAVPRAF2+GFP virus. After 4weeks recovery, mice locomotor activity was recorded in their home cage. Note the contralateral (to the injection site) pivoting behavior and the hyperactivity of the mice.

(**Movie S1b**) For comparison, locomotor activity in control mice injected with the AAV-GFP virus.

Supplementary Experimental Procedures

Animals. Adult male Sprague Dawley rats (250–300 g body weight) were housed in agreement with the institutional guidelines for use of animals and their care, in compliance with national and international laws and policies (Council directives no. 87-848, October 19, 1987, “Ministère de l’Agriculture et de la Forêt, Service Vétérinaire de la Santé et de la Protection Animale”, agreement N° 75-974 to M.D., 75-976 to M.B.E). Wildtype 129S2 mice (8-10 week old) used in these experiments were in a 129S2/SvPas (129S2) background (Charles River, France). Only male were used in all experiments. The GB1 knockout, GB1-floxed mice and their control littermates were from the laboratory of B. Bettler and generated on a BALB/c background [1]. Behavioral tests and animal care were conducted in accordance with the standard ethical guidelines (National Institutes of Health; European Communities Directive 86/609 EEC). All mice were maintained on a 12 light / 12 dark schedule (lights on at 8:00 am), and housed in groups of 3-5 of the same genetic background and sex after weaning. Behavioral studies were carried out between 9:00 am – 3:00 pm). Mice were moved to the testing room in their home cage at least 5 days prior to testing to allow habituation to the environment and stayed there until the end of the experiments. Mice were randomly assigned to different experimental groups. Groups were of 4 to 10 animals and independent experiments were performed 2 to 3 times. Each time, the observer was blind to experimental conditions being measured.

AAV-mediated local VTA PRAF2 or CRE expression. Adeno-associated virus (AAV9)-expressing GFP ($7{,}5 \times 10^{12}$ virus molecules/ml), PRAF2 (IRES) GFP (8×10^{12} virus molecules/ml) or CRE-GFP ($\times 10^{12}$ virus molecules/ml) under the control of the synapsin promoter (UNC Vector Core, Dr. R. Jude Samulski, Chapel Hill) were stereotaxically injected into VTA. Depending of the experiment, 200 nL or 500 nL of

the viral solution was injected. Mice were anesthetized with ketamine (50 mg/kg) and xylazine (2 mg/kg) and fixed in a stereotaxic apparatus. A burr hole was drilled above the VTA (coordinates: 3.5 mm posterior to bregma, 0.5 lateral to midline). Stereotaxically guided injections were made through the hole in the dorsal surface of the cranium (3.5 mm deep). Glass capillary tubes were pulled (HEKA pipette puller PIP5) and tips broken to 40 µm diameter. After 4 weeks recovery and viral expression, the VTA AAV-injected mice were used for behavioral testing or biochemical experiments. Proper viral infection was verified by GFP detection on brain fixed sections. For in vitro studies, hippocampal neurons (DIV 2-3 after plating) were infected with 1µl/ml AAV-PRAF2+GFP and incubated 15 days before the experiments.

Basal Locomotor activity and psychostimulant challenge recording. Locomotor activity was measured in a circular corridor with four infrared beams placed at every 90° (Imetronic, France). Counts were incremented by consecutive interruption of two adjacent beams (i.e., mice moving through one-quarter of the corridor). Mice were intraperitoneally (i.p.) injected with a saline solution and individually placed in the activity box for 60 min during 3 days consecutively for habituation before all behavioral motor experiments. Amphetamine (3mg/kg) induced-locomotor activity in AAV/injected mice was recorded during two hours. Saline or baclofen (4 mg/kg) injections were made thirty minutes before amphetamine challenge. Based on initial trials showing that baclofen completely (4 and 5 mg/kg; i.p) or partially (2,5 and 3 mg/kg) blocked amphetamine-induced locomotion in mice (Sv129 background) and had no effect on basal locomotor activity, we used the 4 mg/kg dose.

Video tracking set up and data analysis. All experiments were performed using a conditioning chamber (30×30×30cm, L×W×H) made with white plastic. A video camera was set 150 cm above four different chambers for simultaneous video recording (640×480 resolution, 30 frames per second). The video files were then processed using ANY-maze software (Stoelting, Wood Dale, IL, USA). The tracking settings were defined in the protocol pane of ANY-maze. The definitions included the white chamber's floor as background. The animal's center-point detection option was selected to track the position of the mice and the tracking frequency was set to 15 frames per second during ten minutes. The animal's center-point was set to be shown on the computer screen, so that the observer could monitor the tracking quality.

Cell Culture. Neuronal cultures were made as described previously [2] with some modifications. Hippocampi of rat embryos were dissected at embryonic day 17-18. After trypsinization, tissue dissociation was achieved with a Pasteur pipette. Cells were counted and plated on poly-D-lysine-coated 15-mm diameter coverslips for immunofluorescence and electrophysiological recording, on 4-well dishes for binding experiments, or on 35 mm dishes for western blots experiments at a density of 300 to 500 cells per square millimeter (depending on the experiment), in complete Neurobasal medium supplemented with B27 (Invitrogen), containing 0.5 mM L-glutamine, 10 U/mL penicillin G, and 10 mg/mL streptomycin. The actual number of surviving neurons was routinely half of the neurons plated, after 7 days in culture. Three hours after plating, the medium was replaced by a conditioned medium obtained by incubating glial cultures (70–80% confluency) for 24 hours in the complete medium described above.

Human Embryonic Kidney 293 (HEK-293) cells, obtained from the ATCC®, were maintained in Dulbecco's modified Eagle's medium, at 37°C in 5% CO2-enriched humidified atmosphere. Media were supplemented with 10% fetal bovine serum (FBS) and 1% Penicillin-Streptomycin. Experiments were conducted on unfrozen batches maintained in culture for no more than five passages. Cells were routinely (every 3 months) screened for the absence of mycoplasma infection using the Lonza, MycoAlert™ Mycoplasma Detection Kit.

Plasmids and transfections. Plasmids coding for Myc-GB1-YFP, HA-GB2, Myc-GB1-Luc were kindly provided by Dr. Michel Bouvier (Institute for Research of Immunology and Cancer, IRIC, University of Montreal, Canada). Myc-GB1-ASA, AA, AA/ASA-YFP were prepared by site directed mutagenesis using Myc-GB1-YFP as template and the QuikChange site-directed mutagenesis procedure (Stratagene). The PRAF2-GFP plasmid was prepared from the PRAF2 cDNA, a generous gifts of Prof. Karin Moelling (Institute of Medical Virology, University Zurich, Switzerland), which was subcloned in frame in the pEGFP-N1 vector (Clontech), Rluc-PRAF2 was generated by subcloning in frame the cDNA for a humanized form of Renilla Luciferase (Biosignal; PerkinElmer Life Sciences) upstream of PRAF2 cDNA. PRAF3 cDNAs were amplified by reverse PCR and subcloned in frame, either in the phRluc-C1 vector encoding the humanized Renilla Luciferase or into the pEYFP-N1 vector (Clontech). HEK-293 cells were transfected using GeneJuice Transfection Reagent (Novagen) according to manufacturer instructions. Hippocampal neurons were transfected using Lipofectamine 2000 (Invitrogen) following manufacturer instructions. PRAF2 cDNA was subcloned in frame in AAV synapsin promoter IRES

GFP plasmid, kindly provided by Dr. Luc Maroteaux and Imane Moutkine (Institut du Fer-à-Moulin, INSERM U839, Paris, France).

Inhibition of Protein Expression by RNA Interference. To silence the expression of PRAF2, hippocampal neurons were transfected with 40nM of each siRNA with Lipofectamine 2000 (Invitrogen) 7 days after plating (DIV7). Two small-interfering RNAs ON-Target plus (S1: 5'-GAUCGAGAGCAUCGGUCUA-3') (S2 : 5'-CUUCACUGCGCCUGAGAAA-3') targeting Rat PRAF2 from Dharmacon (Thermo Fisher Scientific, Inc.), were used. An off-target siRNA (siCONTROL siRNA from Dharmacon) were used as controls. Assays were performed 7 days after the transfection and efficacy of knockdown was assessed by immunoblotting using whole cell lysates.

Antibodies, Drugs, and Receptor Ligands. The following monoclonal antibodies (mAb) or polyclonal antibodies were used for immunofluorescence labeling, FACS analysis or immunoblotting: Anti-PRAF2 rabbit polyclonal antibody (Bioworld Technology Inc, JM4/PRAF2, #L166), Anti-GABA B receptor 1 mouse monoclonal antibody (abcam, #ab55051), Anti-GABA B receptor 2 (N-terminal) rabbit polyclonal antibody (sc-28792, Santacruz biotechnology) Anti-GABA B receptor 2 (C-terminal) rabbit polyclonal antibody (ab75838, Abcam), anti-GM130 mouse monoclonal antibody (BD Biosciences), anti-KDEL mouse monoclonal antibody (10C3, Stressgen), anti-calnexin goat polyclonal (C-20, Santa-Cruz Biotechnologies), anti-myc mouse monoclonal antibody (clone 9E10, Roche), anti-HA (hemagglutinin) monoclonal rat antibody (clone 3F10, Boehringer Mannheim), anti-GFP mouse monoclonal antibody (clones 7.1 and 13.1, Roche), anti-V5 antibody (Invitrogen;

R96025). Dr. Patricia Gaspar (Institut du Fer-à-Moulin, INSERM U839, Paris, France) kindly provided the rabbit polyclonal anti-tyrosine hydroxylase (TH) antibody. The following secondary antibodies were used for immunofluorescence labeling, immunoblotting or FACS analysis: anti-mouse IgG (H+L), anti-rabbit IgG (H+L) and anti-rat IgG (H+L) coupled to Horse Radish Peroxidase (Jackson ImmunoResearch Laboratories), and anti-mouse IgG (H+L) and anti-rabbit IgG (H+L) and anti-goat IgG (H+L) coupled to Alexa-488, Alexa-568 or Alexa-647 (Invitrogen) and Cy5 (Rockland). [3H]CGP 54626 was purchased from ARC (American Radiolabeled Chemical Inc.) and CGP 54626 hydrochloride was purchased from Tocris Bioscience. Coelenterazine h, the substrate of Renilla luciferase was from Interchim (France). D-amphetamine (Sigma-Aldrich, Saint-Quentin Fallavier, France) and baclofen (Tocris Bioscience, USA) were slowly dissolved in 0.9% (wt/vol) NaCl solution (saline). All drugs were administered i.p. (0.1ml/10g body weight).

Immunofluorescence experiments (cell culture). Hippocampal neurons coverslips were proceed for immunofluorescence at DIV8. After 2 washes with PBS+ (Containing 0.1 mM $CaCl_2$ and 0.1 mM $MgCl_2$) at 37°C, cells were fixed for 20 min at room temperature in PBS containing 4% PFA and 4% Sucrose and permeabilized for 5 min in PBS containing 0.2% Triton X-100. Cells were incubated with primary antibodies at the recommended concentration in PBS containing 3% BSA for 1 hr. After 3 washes in the same buffer, Alexa-conjugated secondary antibodies as indicated in figure legends, were added for 1 hr. HEK-293 cells growing on coverslips were fixed in 4% PFA-PBS and quenched with 50 mM NH4Cl for 10 min. A 1% BSA-0.2% Triton X-100-PBS solution was used to block and permeabilize cells. Cells were incubated with primary and Alexa-conjugated secondary antibodies. Coverslips were

mounted in DAPI-containing medium (SlowFade Gold antifade reagent). Image acquisition was performed on a laser-scanning confocal spinning-disk microscope (63X oil immersion lens) equipped with a CoolSnap HQ2 CCD or a wide-field microscope Zeiss Axiovert. Images were collected using the Metamorph Application and were processed with the Image J 1.43u software. Co-localization analyses were done with the Image J plugin JACOP using person's coefficient or overlap coefficients K1&K2. For triple co-localization analysis, co-localization clusters from PRAF2-V5 (blue) and GB1-GFP (green) were first generated with a co-localization plugin (Pierre Bourdoncle, Institut Cochin) generating 8bits images only including co-localized points. The « co-localized points » images and the BIP red channel were then processed with the JACOP plugin to quantify the co-localization of PRAF2/GB1 in the RE.

Tissue preparation and immunofluorescence. Mice were anesthetized with pentobarbital (30 mg/kg, i.p.; Sanofi-Aventis) and perfused transcardially with 4% (w/v) paraformaldehyde in 0.1 M sodium phosphate buffer, pH 7.5. Brains were postfixed overnight in the same solution and stored at 4°C. Fifty-micrometer-thick sections were cut with a Vibratome (Leica) and stored at –20°C in a solution containing 30% (v/v) ethylene glycol, 30% (v/v) glycerol, and 0.1 M sodium phosphate buffer, until they were processed for immunofluorescence. Brain regions were identified using a mouse brain atlas. Sections were incubated overnight with primary antibody (PRAF2 or TH) in PBS, 0,5% Triton, 3% BSA solution at 4°C. Sections were then washed in PBS solution and incubated two hours with secondary antibody (Alexa 647-conjugated antibodies, 1:1000, invitrogen). Finally, sections were cover-slipped in anti-fading mounting medium (moviol-DABCO 25 mg/ml).

Immunofluorescence analysis. Confocal microscopy and image analysis were performed at the Institut du Fer-à-Moulin Imaging Facility. Labeled images from each region of interest were obtained bilaterally using sequential laser-scanning confocal microscopy (Olympus Fluoview). Optical density from isolated neuron was measured with image-J. The regions of interest were drawn as a circle of 2 µm diameter. Specific background values in the extracellular space were subtracted for each cytoplasmic optical density measure.

BRET assays. BRET-donor saturation assays allow establishing the specificity of the interaction between BRET partners (shape of the saturation curve) and the $BRET_{50}$ value (see below), which reflects the propensity of their interaction. Maximal BRET values ($BRET_{max}$), which depend on the distance and on the relative orientation of BRET donor and acceptor, provide little information in the present context where different proteins are compared. The expression level of the BRET-donors, determined in preliminary studies, was the lowest amount of expressed proteins compatible with detectable and robust BRET signals. Based on this, HEK-293 cells were seeded at a density of 500,000 cells/well of a 6-well plate and were transfected with DNA constructs coding for BRET donors and increasing amounts of the BRET acceptor plasmids or BRET competitor plasmids in the case of BRET displacement experiments. The total amount of transfected DNA was maintained constant by adding appropriate amounts of empty vector DNA. Cells were washed (PBS), detached (PBS-EDTA 10mM), centrifuged (1,200 x g for 5min) and resuspended in Hank's-balanced salt solution. After addition of the luciferase substrate, coelenterazine h (5 µM/10^5 cells), luminescence and fluorescence were

measured (see below) by using the Mithras fluorescence-luminescence detector (Berthold Bad Wildbad, Germany). BRET ratios were calculated as described previously [38]. Briefly, the BRET ratio is the fluorescence signal (filter 530±12.5 nm) over the Rluc signal (filter 485±10 nm) measured simultaneously. The readings were repeated three to six times to obtain average values. The specific BRET ratio was calculated by subtracting from the mean BRET ratio value above the background BRET ratio, which corresponds to the signal obtained with cells expressing the BRET-donor alone (not expressing the BRET-acceptor). BRET results were expressed in milli-BRET units (mBRET) by multiplying the values x 1,000 and plotted as a function of YFP/Rluc, in which YFP represents the actual amount of expressed BRET acceptor and Rluc the amount of BRET donor in each sample. To quantify the amount of BRET-acceptor in each well, the fluorescence was measured at 530±12.5 nm after external excitation at 480 nm. To normalize the background fluorescence and luminescence values from experiments conducted in different conditions (different times, different constructs), BRET saturation curves were obtained by plotting BRET values as a function of [(YFP-YFP0)/YFP0] / [Rluc/Rluc0, indicated YFP/Rluc in the figures] where YFP is the specific fluorescence associated with the BRET acceptor in each sample, YFP0 corresponds to background fluorescence measured in cells not expressing the BRET-acceptor, Rluc is the luminescence value associated with the BRET donor in each sample and Rluc0 to the average luminescence value in cells expressing the BRET-donor alone. The amount of BRET-donor in each well was controlled by measuring luminescence values at 485±10 nm after coelenterazine h addition. In case of significant variation (difference of 30% or more from the average value) the corresponding experimental points were excluded from the final plot. Data were fit using a non-linear regression equation assuming a

single binding site (GraphPad Prism) to estimate $BRET_{max}$ and $BRET_{50}$ values (the YFP/Rluc value for half-maximal BRET). In some experiments the BRET saturation experiments were conducted in the presence of variable concentrations of competitors, all the other experimental conditions remaining unchanged.

Receptor cell-surface export analysis. To study the impact of PRAF2 co-expression on GB1 targeting at the cell surface, HEK-293 cells were seeded at a density of 500.000 per well in the appropriated culture medium and were transiently cotransfected with increasing concentrations of HA-GB2 or Luc-PRAF2 and a construct coding for GB1 wild type displaying the myc epitope at the N-terminus and fused C-terminally to the YFP. Empty vector, pCDNA3.1 was used to maintain identical the total amount of transfected DNA. 48 h after transfection, cells were harvested. The level of expression of the constructs was measured by FACS, immunoblotting or luciferase assay. Typically 70-80% of the transfected cells expressed myc-GB1-YFP; in the case of lower % of transfected cells the samples were not analyzed further. To determine cell surface GB1 expression, cell aliquots were stained with a primary antibody directed against the extracellular myc epitope and a CY5-labeled secondary antibody. After washing and fixation in 2% PFA, GB1 cell surface was analyzed by Cytomycs FC500 FACS analyzer (Beckman Coulter). For each point of transfection, 10.000 cells were sorted. A representative example of analysis and calculation is shown in the Supplementary Figure 4.

Binding assay. Quantification of GB1 sites at the surface of rat primary hippocampal neurons was performed with radioligand binding assays. Briefly, rat hippocampal neurons were transfected with siRNAs directed against PRAF2 (S1, S2) or scrambled control at DIV 7-8. For AAV-PRAF2+GFP infection, neurons were infected

at DIV 2-3 with 1 µl/ml of viral solution. One or two weeks after transfection or infection, respectively, neurons were incubated for 20 min at RT in 0.25 mL of binding buffer (120 mM NaCl, 50 mM Tris/HCl, pH 7.4, 5 mM $MgCl_2$, 1mM EDTA) containing 20 nM [^{3}H]CGP54626 (60 Ci/mmol). Non-specific binding was determined in the presence of 10µM unlabeled CGP54626 hydrochloride. After 3 ice-cold washes with the binding buffer, the membrane bound [^{3}H]CGP54626 was recovered by incubation for 10 min at 37°C in 0.2 mL of 0.5 M NaCl, 0.2 M acetic acid buffer, then transferred into plastic vials containing 4.5mL of Aquasolv scintillation fluid (New England Nuclear, Boston, MA, USA) for radioactivity counting. Data were normalized to control siRNA-treated cells or AAV-GFP infected cells and analyzed using GraphPad Prism software.

Binding assays were also performed on membranes, prepared from GB1-GFP or GB2-GFP transfected HEK-293 cells (grown in 10 cm diameter dishes), expressing equivalent amounts of recombinant receptors. After a single wash with PBS, cells were scraped in 10 ml of PBS on ice, centrifuged for 5 min at 1,000 x g. Pellets were dissociated mechanically, lysed in 2 ml of binding buffer (50 mM Tris HCl, 10 mM MgCl2, 0.1 mM EDTA, pH 7.4) and centrifuged for 30 min at 10,000 x g. Membrane-containing pellets were resuspended in binding buffer. Binding assays were performed in the wells of 96-well pates (250 µl per well, final volume) containing 100 µg of membranes, 20 nM (final concentration) of [^{3}H]CGP54626 (60 Ci/mmol) and increasing concentrations of unlabeled CGP54626 hydrochloride. Membranes were harvested by rapid filtration onto Whatman GF/B glass fiber filters (Whatman) pre-soaked with cold saline solution, washed three times with ice-cold buffer, and filters were processed as above. Three independent experiments were performed in duplicate.

Deglycosylation Experiments.

Endoglycosidase H (Endo H) and N-glycosidase F (PNGase F) were purchased from New England Biolabs. All necessary buffers and reagents (NP-40) were supplied. Manufacturer's instructions were followed for the enzymatic digestion. However, due to the aggregation tendency of GB1 receptor above 70°C, denaturation reactions were carried out at 70°C. Briefly, total protein lysates of transfected HEK293 cells were denatured in 0.5% SDS and 40 mM DTT for 10 min at 70 °C and then digested with Endo H overnight at 37 °C, in 50 mM sodium acetate, pH 6. Digestion of denatured proteins with PNGase F was performed in 0.05 M Tris buffer, pH 8.0, supplemented with 1% Nonidet P-40. Digestions were terminated by adding electrophoresis sample buffer. After elution from protein G-Sepharose with 0.5% SDS and 40 mM DTT for 10 min at 70 °C, GB1 receptor co-immunoprecipitated with PRAF2 was treated as the total lysates.

Electrophysiology. *On hippocampal cells in culture.* On the day of recording, the culture medium was replaced with patch-clamp bath solution at least 10 min before recording. All recordings were performed at room temperature on hippocampal neurons at DIV 14. The recorded neurons were continuously perfused at a rate of 2 mL/min throughout the experiment with gassed (95% O2, 5% CO2) bath solution. The patch pipettes were made of thin-walled borosilicate glass capillaries with a BB-CH horizontal pipette puller (Mecanex, Geneva, Swiss). The initial input resistance of the recording pipettes was 3-6 MΩ. To record action potentials, pipettes were filled

with 140 mM K-gluconate, 3 mM EGTA, 1 mM $MgCl_2$, 10 mM HEPES, 2 mM ATP-Mg, pH 7.3 (adjusted with 1M KOH), 290-300 mOsm/L. The bath solution consisted of 124mM NaCl, 3 mM KCl, 2 mM $CaCl_2$, 1 mM $MgSO_4$, 1.25 mM NaH_2PO_4, 26 mM $NaHCO_3$, 10 mM Glucose, pH 7.3, 300-310 mOsm/L. Coverslips containing the neurons were fixed on a chamber mounted on the stage of an upright microscope (Leica DM LFSA, Germany). After obtaining a high-resistance gigaohm seal and achievement whole-cell access, action potentials were recorded at room temperature using an Axopatch 1D amplifier (Axon Instruments, Union City, CA, USA), digitized using a Digidata 1200 interface (Axon Instruments) and stored on a computer. The pClamp6 software from Axon Instruments (Fetchex 6.0.4 for action potential recording) was used to drive storage of current data into data files. Whole cell capacitance and series resistance (using only cells with <30 MΩ) were compensated (>80%) before experimentation. The change in series resistance over the course of each recording was monitored, and recordings with a greater than 20% change in series resistance were excluded from the final data analysis. Off-line analysis was performed using Mini Analysis Program version 6.0.7 (Synaptosoft) and Microsoft Excel software.

In VTA slices. C57Bl6 mice of 3 to 4 weeks old were stereotactically injected unilaterally in the VTA with AAV-GFP control or AAV-Praf2-GFP virus. After three weeks, mice were tested for their locomotor activity and the same mice were anesthetized (Ketamine/Xylazine) and decapitated for slice physiology. Subsequently the brain was isolated and horizontal slices of 250 µm thickness containing the VTA were prepared in ice-cold carbogenated (95% O_2 / 5% CO_2) slicing medium of the following composition (in mM): cholineCl (110); glucose (25); $NaHCO_3$ (25); $MgCl_2$ (7); ascorbic acid (11.6); Na^+-pyruvate (3.1); KCl (2.5); NaH_2PO_4 (1.25); $CaCl_2$ (0.5).

Afterwards slices were allowed to recover in the same medium at 30 °C for 10 minutes before being stored at room temperature in 95% O_2/5% CO_2-equilibrated artificial cerebrospinal fluid (ACSF) containing (in mM): NaCl 124; $NaHCO_3$ 26.2; glucose 11; KCl 2.5; $CaCl_2$ 2.5; $MgCl_2$ 1.3; NaH_2PO_4 1. Slices were kept at 30–32 °C in a recording chamber superfused with 2.5 ml/min ACSF. GFP positive neurons in the VTA were identified using an upright microscope connected to an LED source at 490 nm (Olympus France; CoolLed, UK). Only putative dopamine neurons were recorded from, as only large (>20 pF) *h*-current positive neurons were selected for experiments. Recordings of the holding current were made in ACSF, using an internal solution containing (in mM): 140 K-gluconate, 5 KCl, 10 HEPES, 0.2 EGTA, 2 $MgCl_2$, 4 Na_2ATP, 0.3 Na_3GTP and 10 sodium creatine-phosphate. $GABA_BR$ currents were evoked by application of 15 µM baclofen (in 1eq of NaOH) and were blocked by 5 µM CGP54626 hydrochloride (dissolved in water) (Tocris Cookson, UK). Data analysis was performed in Igor Pro-6 (Wavemetrics, USA). Differences in baclofen-induced $GABA_BR$ currents between the two groups were statistically assessed using a Students T test on the amplitude of both the maximally evoked current, and on the stable steady-state current. Compiled data are expressed as mean ± s.e.m.

Immunoprecipitation of membrane proteins from rat brains. Whole brains of adult male Sprague Dawley rats were homogenized in a Dounce homogenizer in sucrose buffer (320 mM sucrose, 1 mM $NaHCO_3$, 1 mM $MgCl_2$, 50 µm $CaCl_2$, Complete protease inhibitors from Roche). Nuclei were first removed by centrifugation at 1,400 × g for 10 min. The membranes were pelleted by centrifugation at 20,000 × g for 20 min, then resuspended during one night under rotation in solubilization buffer (400 mM NaCl, 10mM Tris, pH 8.0, 1% Triton X-100,

protease inhibitors). The insoluble material was removed by ultracentrifugation (100,000×g for 60min). The resulting supernatant represents the solubilized membrane protein fraction. Twelve mg of solubilized membrane proteins were incubated with anti-PRAF2 antibody or control IgG under rotation overnight. The immune complexes were incubated for 4hrs with 40µl of protein-A sepharose (GE Healthcare). After centrifugation, (13000xg, for 5min) the immunoprecipitated material was washed 3 times with 0.5mL of solubilization buffer, then eluted in Laemmli buffer and separated on 10% SDS-PAGE gels. After transfer on nitrocellulose (PORTRAN, Whatman) blots were probed with the appropriate antibodies. Immunoblots were revealed by luminescence (ECL-plus; GE Healthcare Life Sciences).

Immunoblot analysis from mice brain and cells in culture. Mice were decapitated and brain regions, including the VTA and the hippocampus were dissected on ice, weighed and homogenized by sonication for 15 s in CHAPS buffer (Tris-HCl 75 mM; EDTA 2mM; MgCl2 12 mM ; CHAPS 10 mM). The extraction volumes were 2 ml for all the structures. Samples were then centrifuged at 12,000 x g for 40 min at 4°C and the supernatants were stored at -80°C before used. The antibody dilutions were 1/1000 and 1/5000 for antibodies against PRAF2 and Tubulin, respectively. Primary antibodies were revealed by Fluoprobes 682 goat anti-rabbit or mouse IgG (Interchim, Montluçon, France) at a 1:5000 dilution. Fluorescent immunocomplexes were detected with Odyssey (LI-COR Biosciences, Lincoln, Nebraska). Quantitation was carried out by measuring the average intensity in regions of interest, using the Odyssey software, and data were analyzed with the Prism 3.02 software (GraphPad Software, San Diego, CA). For the experiments aimed at determining the efficacy of

siRNA-dependent knockdown, whole cell lysates were washed with ice-cold PBS and lysed with in 1mL of cold lysis buffer (50 mM Hepes, pH 7.4, 250 mM NaCl, 2 mM EDTA, 0.5% NP-40, 10% glycerol supplemented with protease inhibitors from Roche) and clarified by centrifugation at 13,000 rpm for 20 min at 4°C. Whole-cell lysates were then boiled and analyzed by SDS-PAGE.

Coimmunoprecipitation experiments from transfected cells. V5-tagged wild-type PRAF2 and YFP-tagged wild-type or mutants (ASA, AA, AA/ASA) GB1 constructs were transfected in HEK cells. After twenty four hours, cells were washed in cold PBS, sonicated and solubilized in lysis buffer [75 mM Tris, 2 mM EDTA, 12 mM MgCl2, 10 mM CHAPS, protease inhibitor cocktail EDTA free, pH 7.4] during 5 hours at 4°C. Lysates were centrifuged at 12,000 g during 30 min at 4°C. Immunoprecipitations were performed using anti-V5 antibody (invitrogen, ref: R96025; 1µg per condition; overnight 4°C incubation) and A/G plus agarose beads (santacruz; sc-2003). Immunoprecipitated proteins and 50-100 µg of total proteins were combined with Laemmli buffer, heated at 70°C for 10 min and run on 12% Bis-Tris gel. Immunoblots were probed with anti-gfp (Roche) and anti-V5 antibodies diluted 1/2000 and immunoreactivity was revealed using secondary antibody coupled to 680nm and/or 800 fluorophores using the Odyssey LI-COR infrared fluorescent scanner. All the Co-IP experiments were conducted on identical amount of proteins (starting material); data were normalized over the quantity of immunoprecipitated PRAF2-V5 and quantity of GB1-GFP or GB2-GFP in the input IB.

Statistics. Data were analyzed by two-way ANOVA repeated measures with virus or drug treatment and time as factors. Behavioral and biochemical assays were

analyzed by two or one-way analysis of variance (ANOVA). Bonferroni or t-test were used for post hoc comparisons depending on the experiment. $P<0.05$ was predetermined as the threshold for statistical significance.

Supplemental References

1. Schuler V, Luscher C, Blanchet C, Klix N, Sansig G, Klebs K *et al.* Epilepsy, hyperalgesia, impaired memory, and loss of pre- and postsynaptic GABA(B) responses in mice lacking GABA(B(1)). *Neuron* 2001; 31: 47-58.

2. Carrel D, Masson J, Al Awabdh S, Capra CB, Lenkei Z, Hamon M *et al.* Targeting of the 5-HT1A serotonin receptor to neuronal dendrites is mediated by Yif1B. . *J Neurosci* 2008; 28: 8063-8073.

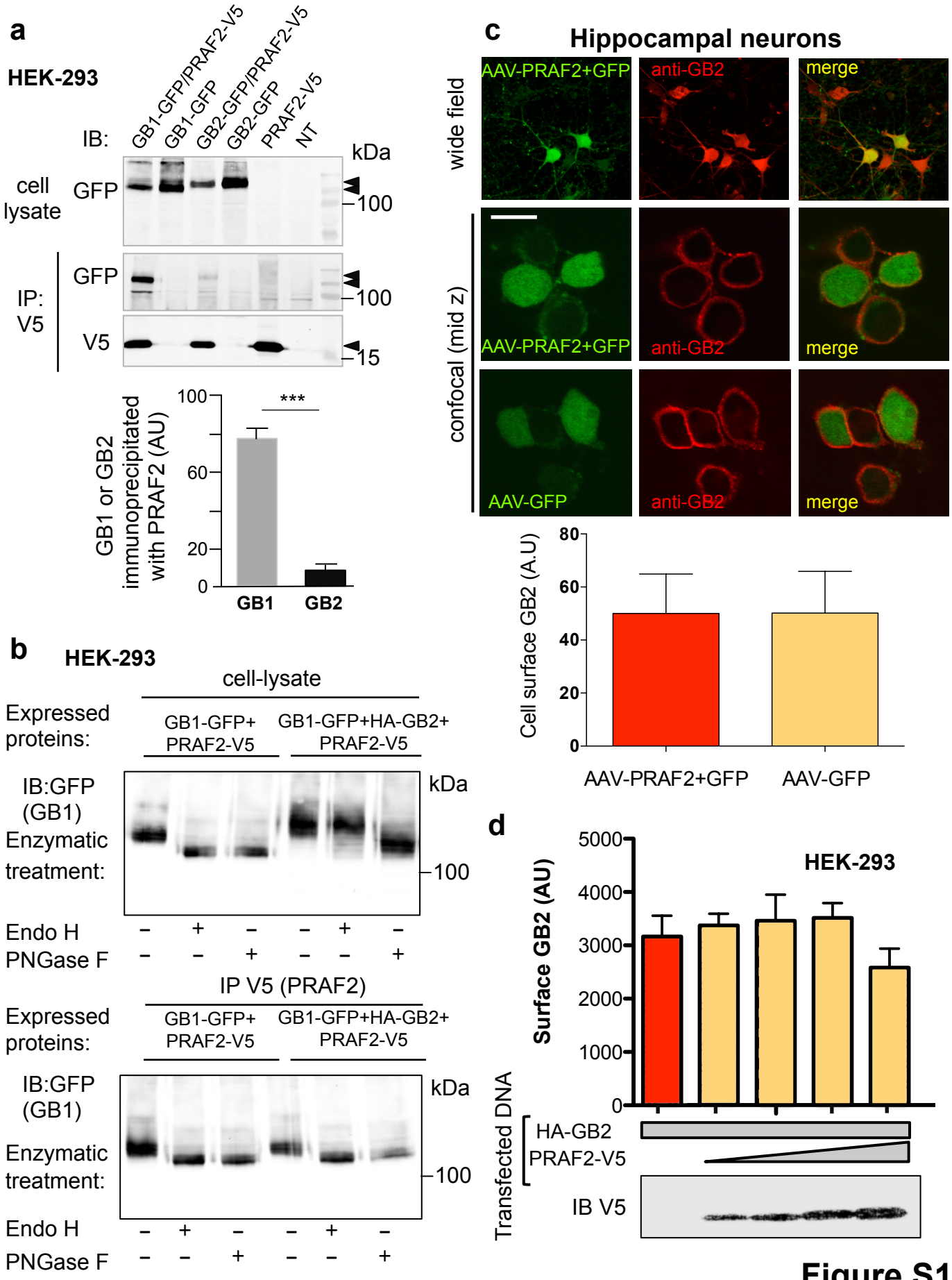
a
HEK-293
GB1-GFP/PRAF2-V5
GB1-GFP
GB2-GFP/PRAF2-V5
GB2-GFP
PRAF2-V5
NT
IB:
kDa
cell lysate
GFP
100
IP: V5
GFP
100
V5
15
GB1 or GB2 immunoprecipitated with PRAF2 (AU)
100
60
20
0
***
GB1
GB2
b
HEK-293
cell-lysate
Expressed proteins:
GB1-GFP+ PRAF2-V5
GB1-GFP+HA-GB2+ PRAF2-V5
IB:GFP (GB1)
kDa
Enzymatic treatment:
100
Endo H
PNGase F
IP V5 (PRAF2)
c
Hippocampal neurons
wide field
confocal (mid z)
AAV-PRAF2+GFP
anti-GB2
merge
AAV-GFP
Cell surface GB2 (A.U)
80
60
40
20
0
d
HEK-293
Surface GB2 (AU)
5000
4000
3000
2000
1000
0
Transfected DNA
HA-GB2
PRAF2-V5
IB V5

Figure S1

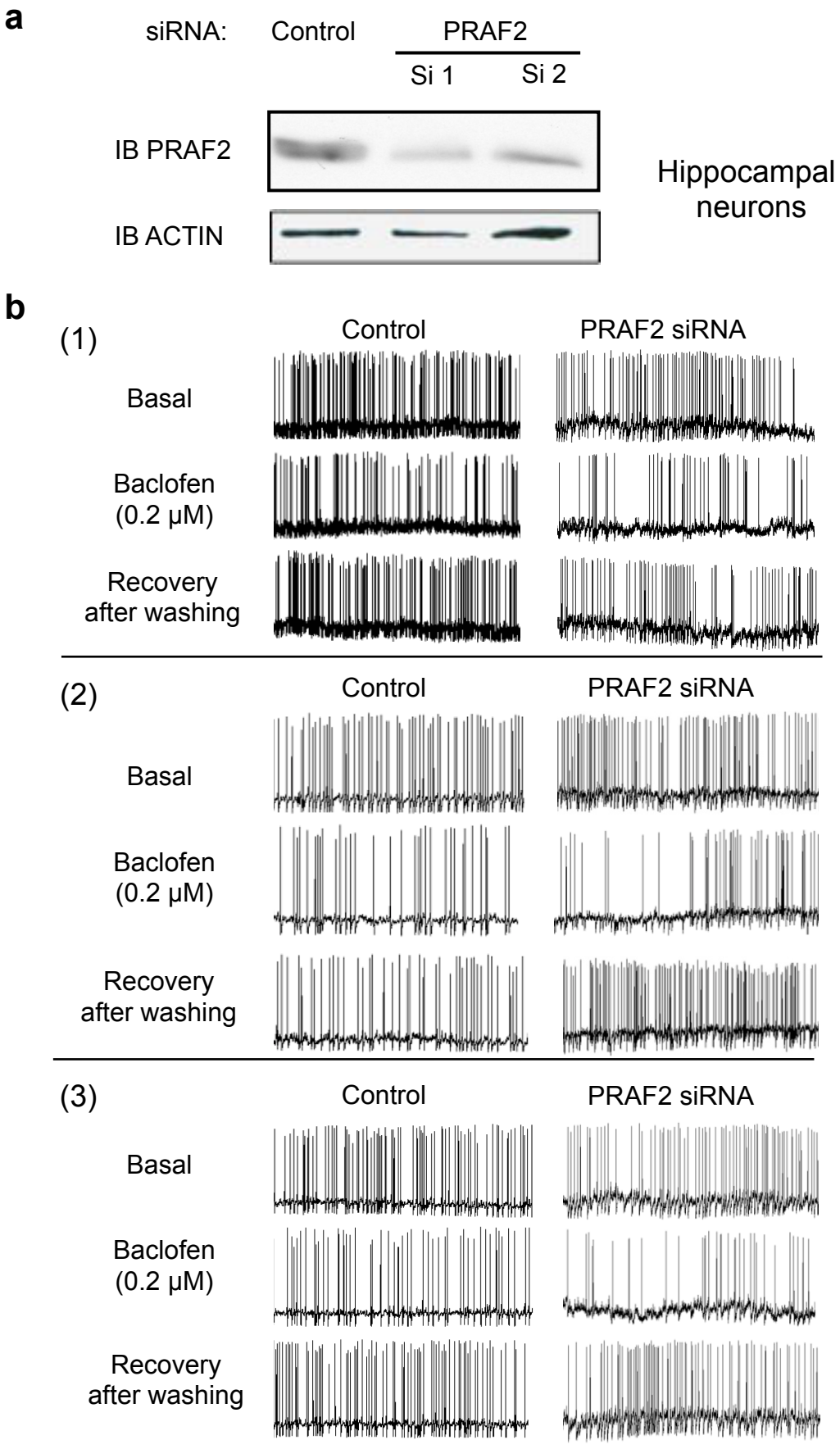
a
siRNA:
Control
PRAF2
Si 1
Si 2
IB PRAF2
IB ACTIN
Hippocampal neurons
b
(1)
Control
PRAF2 siRNA
Basal
Baclofen (0.2 μM)
Recovery after washing
(2)
Control
PRAF2 siRNA
Basal
Baclofen (0.2 μM)
Recovery after washing
(3)
Control
PRAF2 siRNA
Basal
Baclofen (0.2 μM)
Recovery after washing

Figure S2

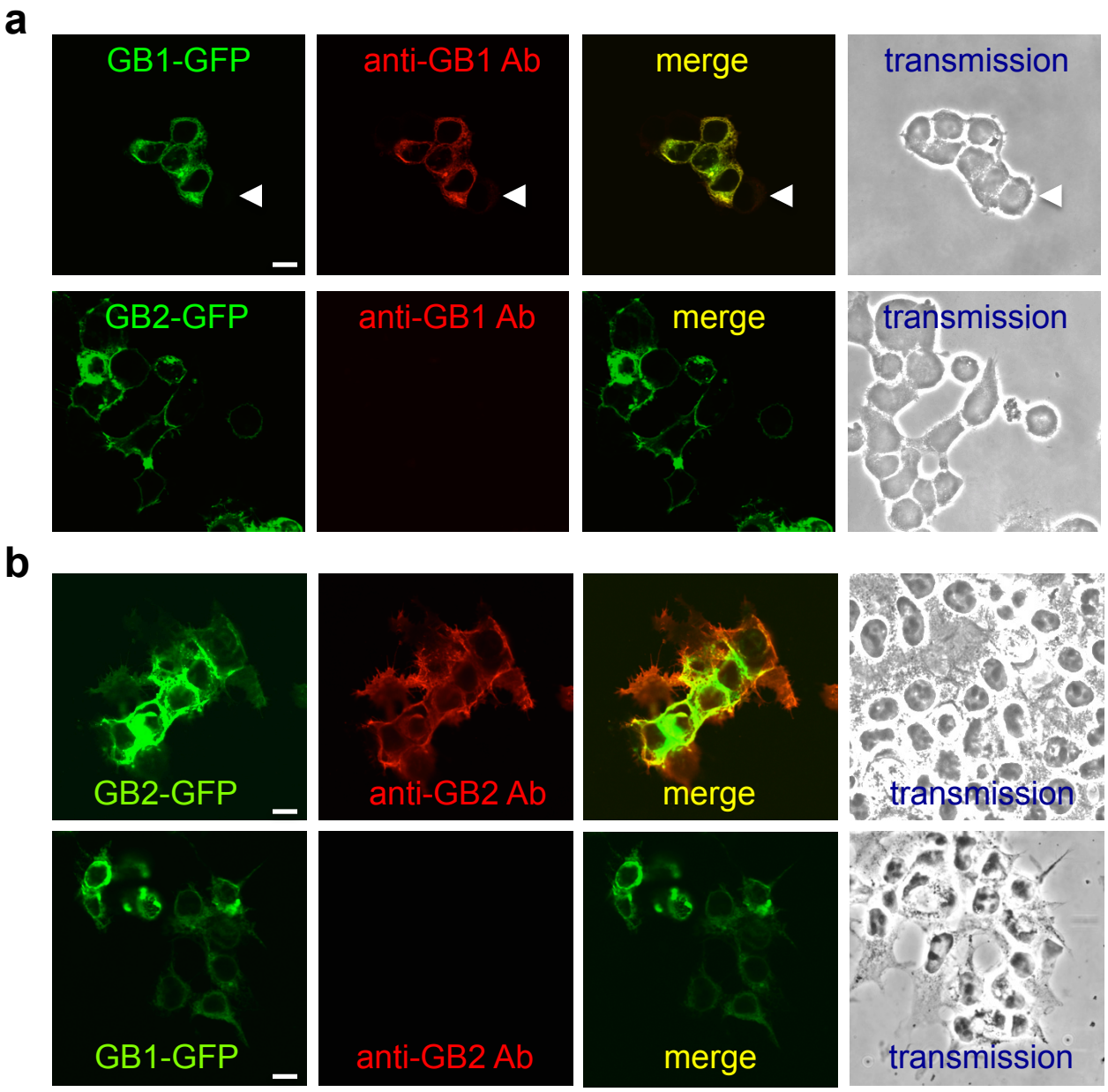
a
GB1-GFP
anti-GB1 Ab
merge
transmission
GB2-GFP
anti-GB1 Ab
merge
transmission
b
GB2-GFP
anti-GB2 Ab
merge
transmission
GB1-GFP
anti-GB2 Ab
merge
transmission

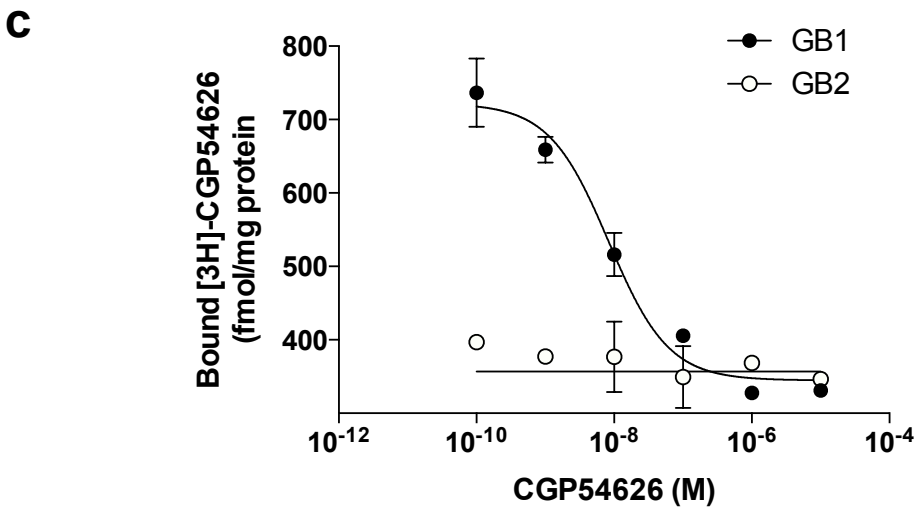
c
GB1
GB2
Bound [3H]-CGP54626 (fmol/mg protein
800
700
600
500
400
10-12
10-10
10-8
10-6
10-4
CGP54626 (M)

Figure S3

Myc-GB1-YFP

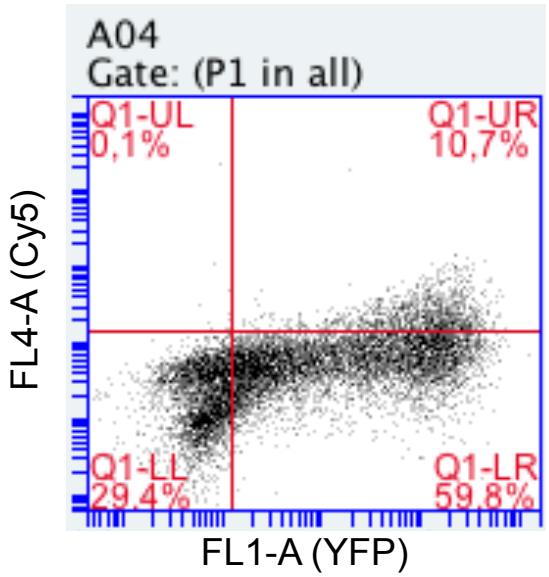

Myc-GB1-YFP+ HA-GB2

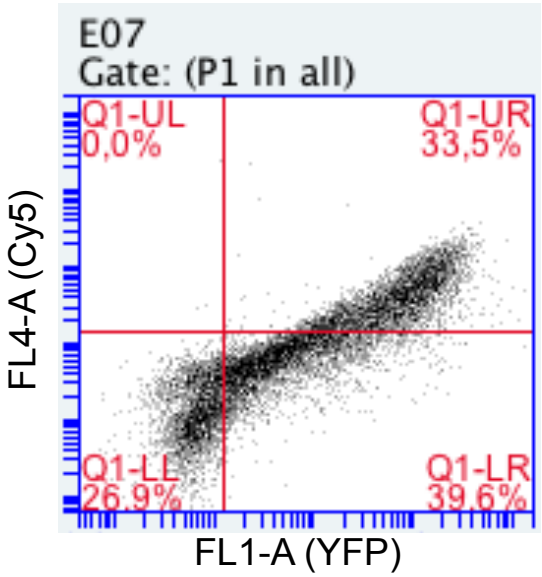

Plot 3: A04: Gated on (P1 in all)	Count	% of This Plot	Mean FL1-A	Mean FL4-A
This Plot	10 000	100,00%	52664,41	779,72
Q1-UL	13	0,13%	974,77	20122,92
Q1-UR	1 072	10,72%	150274,57	942,27
Q1-LL	2 936	29,36%	652,23	262,21
Q1-LR	5 979	59,79%	40816,73	603,42

Plot 3: E07: Gated on (P1 in all)	Count	% of This Plot	Mean FL1-A	Mean FL4-A
This Plot	10 000	100,00%	41316,78	2175,69
Q1-UL	4	0,04%	924,75	61497,00
Q1-UR	3 348	33,48%	108604,78	5498,88
Q1-LL	2 691	26,91%	668,46	179,93
Q1-LR	3 957	39,57%	12069,01	661,97

Q1-LL: nontransfected cells (group 1)
Q1-LR: YFP positives cells (group 2)
Q1-UL: Cy5 positives cells (group 4)
Q1-UR: YFP and Cy5 positives cells (group 3)

Figure S4

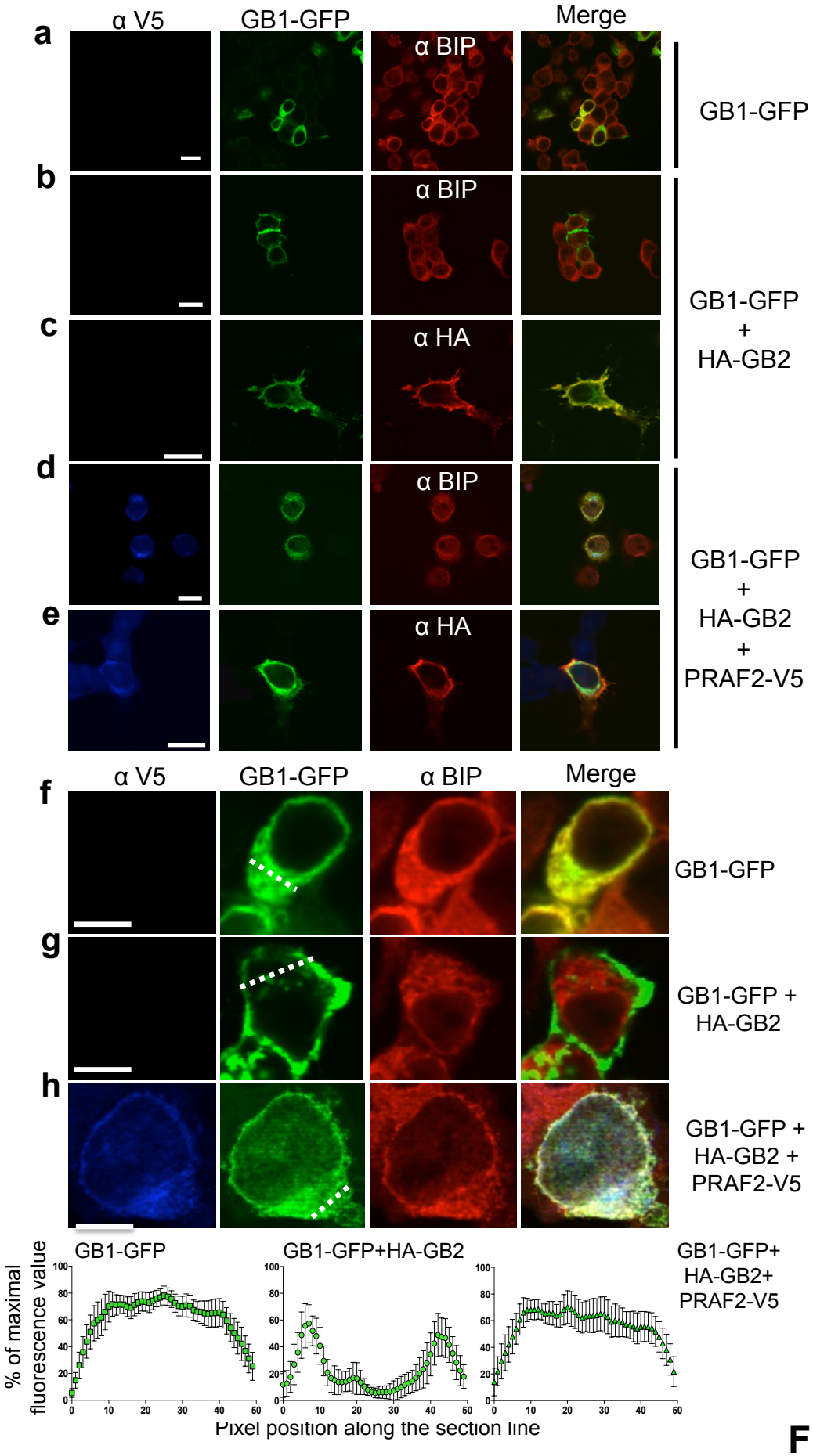
a
b
c
d
e
f
g
h
α V5
GB1-GFP
α BIP
Merge
α HA
GB1-GFP
GB1-GFP + HA-GB2
GB1-GFP + HA-GB2 + PRAF2-V5
GB1-GFP
GB1-GFP+HA-GB2
GB1-GFP+ HA-GB2+ PRAF2-V5
% of maximal fluorescence value
Pixel position along the section line

Figure S5

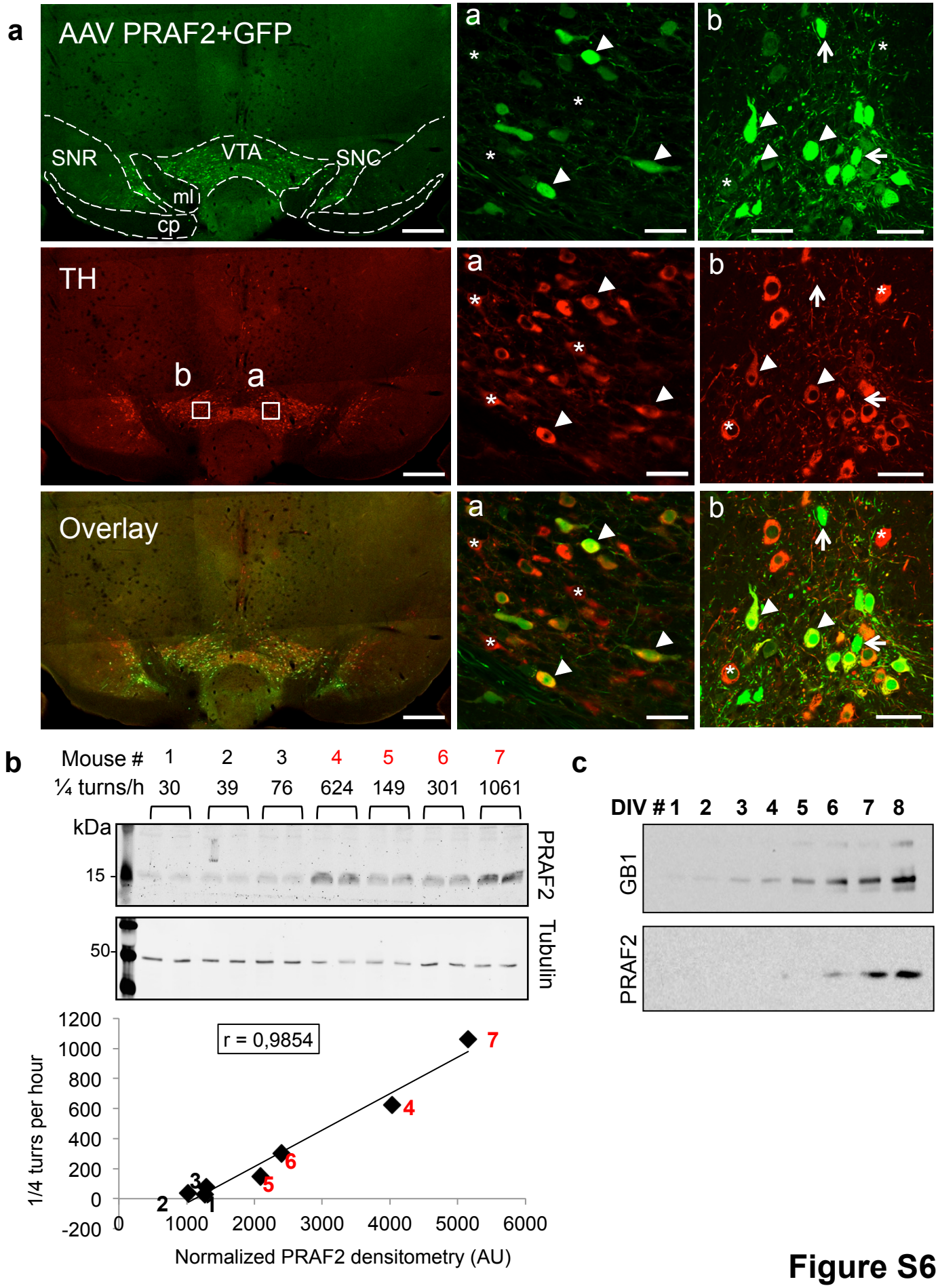
a
AAV PRAF2+GFP
SNR
VTA
SNC
ml
cp
TH
b
a
Overlay
a
b
b
Mouse # 1 2 3 4 5 6 7
¼ turns/h 30 39 76 624 149 301 1061
kDa
15
50
PRAF2
Tubulin
r = 0,9854
1/4 turrs per hour
Normalized PRAF2 densitometry (AU)
c
DIV # 1 2 3 4 5 6 7 8
GB1
PRAF2

Figure S6

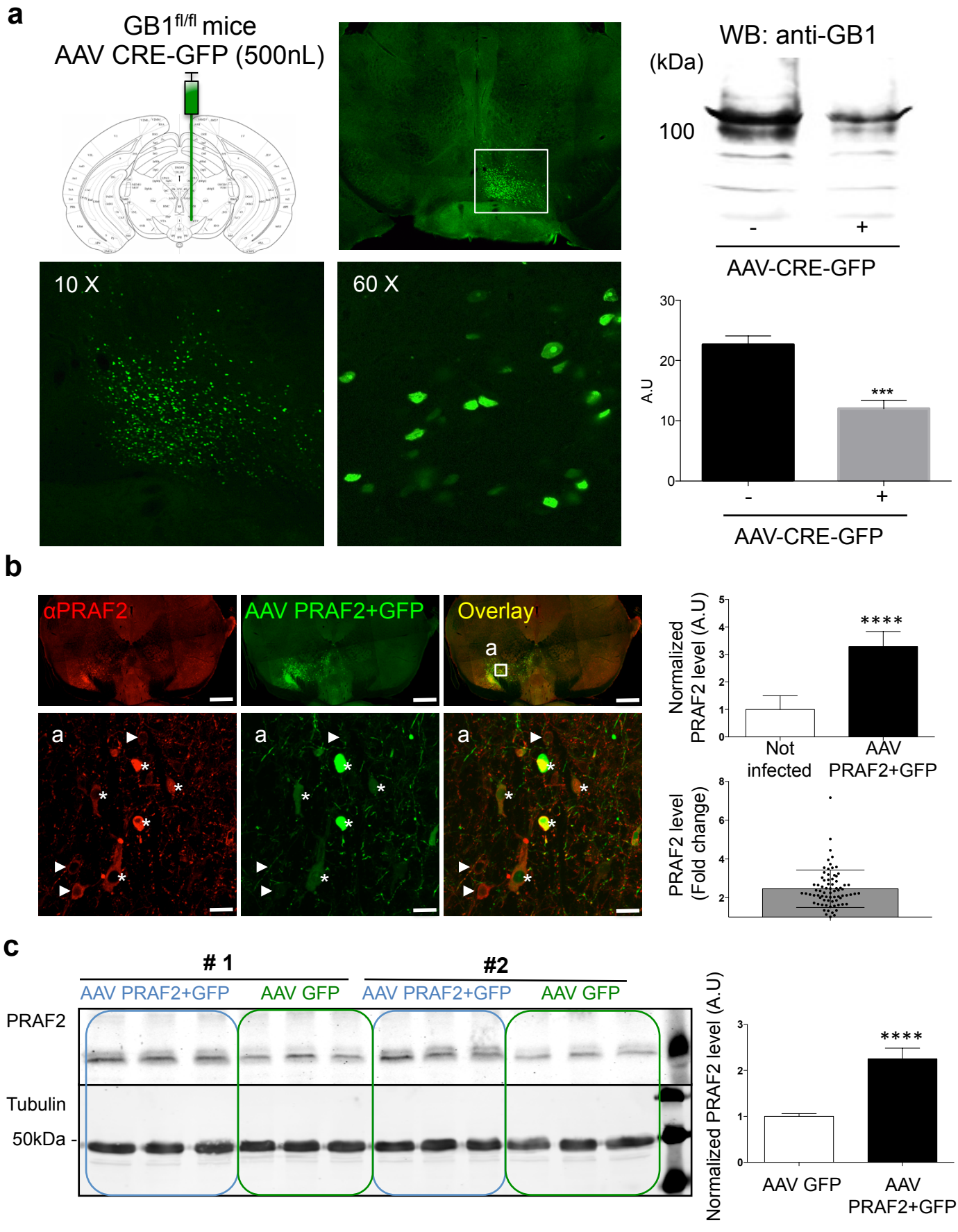
a
GB1fl/fl mice
AAV CRE-GFP (500nL)
10 X
60 X
WB: anti-GB1
(kDa)
100
-
+
AAV-CRE-GFP
30
20
10
0
A.U
***
-
+
AAV-CRE-GFP
b
αPRAF2
AAV PRAF2+GFP
Overlay
a
Normalized PRAF2 level (A.U)
****
Not infected
AAV PRAF2+GFP
PRAF2 level (Fold change)
c
1
#2
AAV PRAF2+GFP
AAV GFP
AAV PRAF2+GFP
AAV GFP
PRAF2
Tubulin
50kDa -
Normalized PRAF2 level (A.U)
****
AAV GFP
AAV PRAF2+GFP

Figure S7

Bonferroni's multiple comparisons test	Mean Diff,	95% CI of diff,	Summary	N1	N2	t	DF
Baclofen 0µM							
untreated vs. Si-control	0	-19,56 to 19,56	ns	12	9	0	137
untreated vs. Si1-PRAF2	0	-18,11 to 18,11	ns	12	12	0	137
untreated vs. Si2-cPRAF2	0	-22,18 to 22,18	ns	12	6	0	137
Si-control vs. Si1-PRAF2	0	-19,56 to 19,56	ns	9	12	0	137
Si-control vs. Si2-cPRAF2	0	-23,38 to 23,38	ns	9	6	0	137
Si1-PRAF2 vs. Si2-cPRAF2	0	-22,18 to 22,18	ns	12	6	0	137
Baclofen 0.04µM							
untreated vs. Si-control	0,3929	-20,70 to 21,49	ns	12	7	0,04986	137
untreated vs. Si1-PRAF2	24,63	4,381 to 44,87	**	12	8	3,256	137
untreated vs. Si2-cPRAF2	9,75	-15,86 to 35,36	ns	12	4	1,019	137
Si-control vs. Si1-PRAF2	24,23	1,277 to 47,19	*	7	8	2,826	137
Si-control vs. Si2-cPRAF2	9,357	-18,44 to 37,16	ns	7	4	0,9011	137
Si1-PRAF2 vs. Si2-cPRAF2	-14,88	-42,04 to 12,29	ns	8	4	1,466	137
Baclofen 0.2µM							
untreated vs. Si-control	0,873	-21,48 to 23,22	ns	7	9	0,1046	137
untreated vs. Si1-PRAF2	40,03	18,17 to 61,89	****	7	10	4,903	137
untreated vs. Si2-cPRAF2	35,26	10,59 to 59,94	**	7	6	3,826	137
Si-control vs. Si1-PRAF2	39,16	18,78 to 59,53	****	9	10	5,144	137
Si-control vs. Si2-cPRAF2	34,39	11,01 to 57,76	***	9	6	3,938	137
Si1-PRAF2 vs. Si2-cPRAF2	-4,767	-27,67 to 18,14	ns	10	6	0,5572	137
Baclofen 1µM							
untreated vs. Si-control	11,86	-11,10 to 34,81	ns	8	7	1,383	137
untreated vs. Si1-PRAF2	33,67	13,42 to 53,91	***	8	12	4,452	137
untreated vs. Si2-cPRAF2	34	8,715 to 59,29	**	8	5	3,6	137
Si-control vs. Si1-PRAF2	21,81	0,7155 to 42,90	*	7	12	2,768	137
Si-control vs. Si2-cPRAF2	22,14	-3,828 to 48,11	ns	7	5	2,283	137
Si1-PRAF2 vs. Si2-cPRAF2	0,3333	-23,28 to 23,94	ns	12	5	0,0378	137
Baclofen 5µM							
untreated vs. Si-control	-4,222	-27,60 to 19,15	ns	9	6	0,4835	137
untreated vs. Si1-PRAF2	11,78	-12,96 to 36,52	ns	9	5	1,275	137
untreated vs. Si2-cPRAF2	9,778	-19,79 to 39,35	ns	9	3	0,8853	137
Si-control vs. Si1-PRAF2	16	-10,86 to 42,86	ns	6	5	1,595	137
Si-control vs. Si2-cPRAF2	14	-17,36 to 45,36	ns	6	3	1,195	137
Si1-PRAF2 vs. Si2-cPRAF2	-2	-34,39 to 30,39	ns	5	3	0,1653	137

Table 1. Statistical analysis of values in Figure 2e